Table2. Primer list that used in this work.

primer name	sequence	description
primer1	GAACATATGTTTGCATGGAGG	to make plasmid for allelic replacement
primer2	CAAGCTCTGGGGCACTAGTT	to make plasmid for allelic replacement
primer3	ATTGTAAAGAGTGAAGGGAG	to construct pTS1303,1304
primer4	AAAGTTGGACAATCTATCCTA	to construct 1301
primer5	AGGATAGATTGTCCAACTTT	to construct pTS1308-1310
primer6	TTTATGGGTAACTATGATGT	to construct pTS1305
primer7	ACTTGTTCCTATCATATGTA	to make CPE1563 probe
primer8	ATTCTTCCTCCGCTGTCACT	to construct pTS1314
primer9	AGTGACAGCGGAGGAAGAAT	to make CPE1562 probe
primer10	ATGGTATTCATACAATATTG	to construct pTS1306
primer11	TTTAAACCTTCACATAAA	to make CPE1562 probe,
primer12	TAGGTATTCCATCTACTAT	sequence primer
primer13	TTTTTCAGCTATTAACTTCGA	to construct pTS1313,1314
primer14	TTTACAGCAAGCATACTTA	to construct pTS1310,1311, to make 1561 probe
primer15	TTCTGGAGGAGCACATTCAG	to construct pTS1302
primer16	TCCTTAGAGTCATACATTGC	to make CPE1561 probe
primer18	TTGTTAAAAACTATAGATTCTT	to check mutation, agrD Northern
primer19	GGCCGGTTTAAAACCTACCT	to check mutation, agrD Northern
primer20	TATACTAGATTAGAGAGGGAGAAT	to make CPE1560 probe
primer21	CTCTTCTCCTCCATATCTAGC	to make CPE1560 probe
primer22	ACTTCAGCTAAGCTATGCTG	to construct pTS1302
primer23	AAGGTCATAGGTGTTGTATAGC	to make plasmid for allelic replacement
primer24	TAACAGTACGTGTTCCAAAC	to construct pTS1301, 1303
primer25	AGATGGGGCGGTAGACGTAG	to make plasmid for allelic replacement

Table1. Strains and plasmids

strains and plasmids	Description	Source or reference
Strains		
C.perfringens		
strain13	wild type strain (typeA)	
TS133	strain13 *virR*:: Tet	
TS230	strain13 Δ*agrBD* Em	this study
TS231	strain13 Δ*agrBD*-Δ*virR* :: Tet , Em	this study
pJIR418	*E.coli*-*C. Perfringens* shuttle vector, Cm, Em	
pTS405	pJIR418 Ω (*Pst*I 4.5 kb strain 13 genomic library) (*virR*'*virS*' complementation vector) Cm	Shimizu, unpublished
pTS1301	pJIR418 Ω (Δpromoter CPE1562-CPE1561-*agrD*-CPE1560)	this study
pTS1302	pJIR418 Ω (Δpromoter *agrD*-CPE1560)	this study
pTS1303	pJIR418 Ω (CPE1563-CPE1562-CPE1561-*agrD*-CPE1560) including promotor	this study
pTS1304	pJIR418 Ω (CPE1563-CPE1562-CPE1561-*agrD*) including promotor	this study
pTS1305	pJIR418 Ω (Δpromoter-CPE1562-CPE1561-*agrD*)	this study
pTS1306	pJIR418 Ω (Δpromoter-CPE1561-*agrD*)	this study
pTS1307	pJIR418 Ω (Δpromoter-*agrD*)	this study
pTS1308	pJIR418 Ω (CPE1562-CPE1561-*agrD*)	this study
pTS1309	pJIR418 Ω (CPE1561-*agrD*)	this study
pTS1310	pJIR418 Ω (*agrD*)	this study
pTS1311	pJIR418 Ω (CPE1563-*agrD*)	this study
pTS1312	pJIR418 Ω (CPE1563-CPE1562-*agrD*)	this study
pTS1313	pJIR418 Ω (CPE1562-*agrD*)	this study
pTS1314	pJIR418 Ω (CPE1562-CPE1561-*agrD*)	this study

JOURNAL OF BACTERIOLOGY, Dec. 2008, p. 7719–7727 Vol. 190, No. 23
0021-9193/08/$08.00+0 doi:10.1128/JB.01573-07

Characterization of Genes Regulated Directly by the VirR/VirS System in *Clostridium perfringens*[▽]

Kayo Okumura,[1]† Kaori Ohtani,[2] Hideo Hayashi,[1] and Tohru Shimizu[2]*

Department of Infection Biology, Institute of Basic Medical Sciences, University of Tsukuba, Tsukuba, Ibaraki 305-8575,[1] and Department of Bacteriology, Graduate School of Medical Science, Kanazawa University, Kanazawa, Ishikawa 920-8640,[2] Japan

Received 29 September 2007/Accepted 1 September 2008

Analysis of the complete sequence of the genome of *Clostridium perfringens* strain 13 resulted in identification of five genes, including *pfoA* (encoding theta toxin) and *vrr* (encoding VirR/VirS-regulated RNA), with consensus VirR-binding sequences upstream of the open reading frame (ORF), suggesting that expression of these genes may be regulated directly by the two-component VirR/VirS system. To test this possibility, we examined VirR/VirS system-mediated transcriptional regulation of three genes, *virT*, *ccp* (encoding alpha-clostripain), and *virU*, with the novel VirR-binding sequences. Northern analysis revealed that the steady-state levels (increases or decreases in the amounts of RNA expressed) of *virT*, *ccp*, and *virU* mRNAs were lower in a *virR* mutant strain than in the wild-type strain, as were the levels of the *pfoA* and *vrr* transcripts. The consensus VirR-binding sites were located similarly relative to the transcription start sites in the *virT*, *ccp*, and *virU* promoters. Mutation and overexpression analyses with *virT* and *virU* revealed that the *virT* gene product has a negative effect on expression of *pfoA* and *ccp*, whereas the *virU* gene product positively affects expression of *pfoA*, *virT*, *ccp*, and *vrr*. Nonsense and frameshift mutations in the *virT* or *virU* putative ORF did not affect the regulatory functions, suggesting that *virT* and *virU* may encode RNA regulators rather than proteins. These results suggest that a complex regulatory network, perhaps involving several regulatory RNA molecules, governs the expression of the VirR/VirS regulon in *C. perfringens*.

The gram-positive anaerobic bacterium *Clostridium perfringens* produces numerous extracellular toxins that are believed to play important roles in the pathogenicity of various diseases, including gas gangrene, which is also known as clostridial myonecrosis (9, 21). Because the toxins are thought to act synergistically in the development of gas gangrene (2), knowledge of the mechanisms that regulate expression of toxin genes is critical for understanding the pathogenesis of myonecrosis.

Bacterial two-component systems, consisting of a sensor histidine kinase and a response regulator, enable bacteria to respond to various environmental conditions through a phosphorelay between the sensor and the regulator. The two-component VirR/VirS system comprising the VirR response regulator and the VirS sensor protein is known to be involved in global regulation of the production of theta-toxin (also known as perfringolysin O), kappa-toxin (or collagenase), alpha-toxin (or phospholipase C), sialidase, protease, and hemagglutinin in *C. perfringens* (13, 24). The VirR/VirS system regulates the mRNA levels of *plc* (alpha-toxin), *pfoA* (theta-toxin), and *colA* (kappa-toxin) (4). Primer extension analysis revealed both VirR/VirS-dependent and independent promoters for *pfoA* and *colA* and a single VirR/VirS-dependent promoter for *plc* (4). The absence of a consensus binding site for phosphorylated VirR protein in the promoters of the *colA* and *plc* genes (4) suggests that complex regulatory networks might be involved in *C. perfringens* toxin production (26).

Four targets of the VirR/VirS system have been identified through differential display analyses. The VirR/VirS system was found to promote expression of *ptp* (encoding protein tyrosine phosphatase), *cpd* (encoding 2′,3′-cyclic nucleotide phosphodiesterase), and *hyp7* (encoding a hypothetical 7-kDa protein) (3) and to inhibit expression of the *ycgJ-metB-cysK-luxS* (*ygaG*) operon (3, 20). It was suggested previously that *hyp7* acts as a secondary regulator that positively regulates the levels of *colA* and *plc* mRNAs but not the level of *pfoA* mRNA (3). However, we reported previously that VirR/VirS-regulated RNA (VR-RNA) (encoded by *vrr*) transcribed from the Hyp7 coding region is a regulatory RNA that mediates the signal from the VirR/VirS system to control the expression of *colA*, *plc*, *ptp*, *cpd*, and *ycgJ-metB-cysK-luxS*, whereas *pfoA* is regulated directly by the VirR/VirS system (28). The VirR/VirS–VR-RNA cascade was also found to affect levels of plasmid-borne *cpb2* (encoding beta2 toxin) and *cna* (encoding a possible collagen adhesin) mRNAs positively and negatively, respectively (19).

Two repeated sequences have been found upstream of the *pfoA* promoter (4), and it was reported previously that the VirR protein binds independently to these two repeats (CCC AGTTNTNCAC) (6). Interestingly, a monomeric repeat similar but not identical to the *pfoA* VirR-binding site has also been found in the promoter of *vrr*, the gene encoding VR-RNA (28). A CCAGTTNNNCAC core motif was highly conserved in both genes. These findings suggest that the VirR protein may bind to the *vrr* promoter, activating transcription of VR-RNA, which in turn activates *colA* and *plc* transcription,

* Corresponding author. Mailing address: Department of Bacteriology, Graduate School of Medical Science, Kanazawa University, 13-1 Takara-Machi, Kanazawa, Ishikawa 920-8640, Japan. Phone: 81-76-265-2201. Fax: 81-76-234-4230. E-mail: tshimizu@med.kanazawa-u.ac.jp.

† Present address: Department of Infectious Diseases, Research Institute, International Medical Center of Japan, 1-21-1 Toyama, Shinjuku, Tokyo 162-8655, Japan.

▽ Published ahead of print on 12 September 2008.

TABLE 1. Bacterial strains and plasmids used in this study

Strain or plasmid	Description[a]	Reference or source
C. perfringens strains		
13	Wild-type strain (type A)	14
TS133	Strain 13 *virR*::Tet^r	24
TS140	Strain 13 Δ*vrr* Em^r	28
TS190	Strain 13 *virT*::Em^r	This study
E. coli DH5α	*supE*44 Δ*lacU169* (ϕ80 *lacZ*ΔM15) *hsdR17 recA1 endA1 gyrA96 thi-1 relA1*	Takara Bio Inc.
Plasmids		
pBT405	pJIR418 Ω(PstI 4.3-kb strain 13 genomic library) (*virR*$^+$ *virS*$^+$ complementation vector), Amp^r	Shimizu, unpublished data
pJIR418	*E. coli-C. perfringens* shuttle vector, Cm^r Em^r	29
pSB1031	pJIR418 Ω(PCR-amplified 637-bp fragment) (*vrr*$^+$ complementation vector)	4
pTS930	pJIR418 Ω(PCR-amplified 1,400-bp fragment) (*virT*$^+$ complementation vector)	This study
pTS931	pJIR418 Ω(PCR-amplified 539-bp fragment) (*virU*$^+$ complementation vector)	This study
pTS932	pTS930 (585T→A)	This study
pTS933	pTS931 (182A→T)	This study
pTS934	pUC118 Ω(PCR-amplified 334-bp fragment) (*virT*$^+$ suicide vector), Em^r	This study
pTS935	pTS930 (1-bp frameshift at position 33)	This study
pTS936	pTS931 (1-bp frameshift at position 15)	This study
pUC19	Cloning vector, Amp^r *lacZ'* pMB 1 *ori*	Takara Bio Inc.
pUC118	Cloning vector, Amp^r *lacZ'* pMB 1 *ori*	Takara Bio Inc.

[a] Tet^r, resistance to tetracycline; Em^r, resistance to erythromycin, Cm^r, resistance to chloramphenicol; Amp^r, resistance to ampicillin.

thus forming the basis for a regulatory cascade in the VirR/VirS regulon (28).

The complete genomic sequence of *C. perfringens* strain 13 has been reported (25). On the basis of sequence similarities with other known virulence genes, more than 20 candidate virulence genes were identified. By screening the genome for the previously identified VirR-binding consensus sequence, we identified genes potentially regulated by the VirR/VirS system. Five genes were found to have the consensus VirR-binding site in their putative promoter regions (25). In the present study, regulation of expression of these novel target genes was analyzed to improve our understanding of the VirR/VirS regulon in *C. perfringens*.

MATERIALS AND METHODS

Strains, plasmids, medium, and culture conditions. The strains and plasmids used in this study are listed in Table 1. All *C. perfringens* strains were cultured in Gifu anaerobic medium (Nissui, Japan) at 37°C under anaerobic conditions as described previously (24). A single-crossover mutation was introduced into the *virT* gene of *C. perfringens* strain 13 with a pUC19-based suicide vector containing a 334-bp internal PCR fragment of *virT* and the *ermB* gene from pJIR418 (29). *Escherichia coli* DH5α was cultured as described previously (22). Plasmids pUC19 and pUC118 were used for cloning in *E. coli*, and pJIR418 (29) was used as an *E. coli-C. perfringens* shuttle vector.

DNA manipulation. Recombinant DNA was manipulated as described previously (22), unless otherwise noted. *C. perfringens* strains were transformed by electroporation as previously described (24).

Northern hybridization. Total RNA from *C. perfringens* was extracted and Northern blotting was performed as previously described (1) with an AlkPhos-direct kit and CDP-*star* chemiluminescence (GE Healthcare). DNA probes were prepared from genomic DNA of *C. perfringens* strain 13 by performing PCR with the appropriate primer sets (Table 2). In some situations, the signal densities of the mRNA bands were measured with a densitometer. All Northern hybridization experiments were performed at least three times, and the reproducibility was confirmed. The results described below are representative results from the repeated experiments.

Primer extension analysis. Primer extension was carried out as described previously (17) by using an Amersham 5′ oligolabeling fluorescence kit and the Promega primer extension system. Oligonucleotide primers 0845-PE, 0846-PE, and 0920-PE used to determine the transcription start sites of CPE0845 (*virT*), CPE0846 (*ccp*), and CPE0920 (*virU*), respectively, are shown in Table 2. Signals were detected with a FluorImager analyzer (GE Healthcare).

Assays for perfringolysin O and alpha-clostripain. The perfringolysin O activity in the *C. perfringens* culture supernatant was measured by the horse erythrocyte hemolysis method described previously (2). *C. perfringens* cells were cultured for 3 h to mid-log phase (see Fig. 2A) and collected by centrifugation. The supernatant was used for the hemolytic assay. Hemolytic activity was expressed as the reciprocal of the dilution that resulted in 50% hemolysis of 0.5% horse erythrocytes. The proteolytic activity of alpha-clostripain in the culture supernatant was determined with azocasein (Sigma Aldrich Japan) and the cysteine protease-specific inhibitors leupeptin and antipain (Wako Pure Chemicals) as previously described (11, 27). In brief, *C. perfringens* cells were cultured for 2 h to early log phase (see Fig. 2A) and collected by centrifugation, and 500 μl of the supernatant was mixed with an equal volume of an azocasein solution (5 mg/ml azocasein in 25 mM Tris-HCl [pH 7.5]–5 mM dithiothreitol) with or without 10 μM leupeptin or antipain. The mixture was incubated for 2 h at 37°C with gentle shaking, intact azocasein was removed by 3% trichloroacetic acid precipitation, and the absorbance at 450 nm of the supernatant was determined.

Site-directed mutagenesis and frameshift mutagenesis. Site-directed mutagenesis of the *virT* gene harbored by pTS930 was performed with an LA PCR in vitro mutagenesis kit (Takara Bio) with the mutagenic primer virT-NM (Table 2) to obtain pTS932. The *virU* gene on pTS931 was mutated by using a QuikChange site-directed mutagenesis kit (Stratagene) with primers virU-NM-F and virU-NM-R (Table 2) to obtain pTS933. Similarly, 1-base deletion frameshift mutations at positions 33 and 15 in the *virT* and *virU* coding regions, respectively, in the complemented plasmid vectors pTS930 and pTS931 (Table 1), respectively, were obtained by using a QuikChange site-directed mutagenesis kit (Stratagene) with primers virT-FM-F and virT-FM-R for *virT* and primers virU-FM-F and virU-FM-R for *virU* to construct pTS935 and pTS936 (Table 1). All procedures were performed according to the manufacturers' instructions.

RESULTS

Screening for VirR-binding sites in the *C. perfringens* genome. We scanned the genomic sequence of *C. perfringens* (25) for VirR-binding sites (CCAGTTNNNCAC) located upstream of the open reading frame (ORF). Only five genes, *pfoA*, CPE0845 (*virT*), CPE0846 (*ccp*), CPE0920 (*virU*), and *vrr*, were found to have sequences similar to the VirR-binding site in their putative promoter regions (Fig. 1) (25). With the exception of *virT* and *ccp*, which are located back to back and are

TABLE 2. Oligonucleotides used in this study

Primer	Sequence (5′to 3′)	Use
virT-F	GAAGGTAAGTACCAAGATGA	Northern blotting
virT-R	TGATATTGCCACCCCAACTT	Northern blotting
ccp-F	GAGGCCGAAAAGACTGAAGG	Northern blotting
ccp-R	GCCCAATGTGGTATTGCTTG	Northern blotting
virU-F	CGATTCGTTTTTGATAGAAATGG	Northern blotting
virU-R	TTTATTTCTAGTTTTTCCTTTGATGA	Northern blotting
vrr-F	GACCAGTTACGCACAAAC	Northern blotting
vrr-R	GGACAGTTCTATTTCTAGG	Northern blotting
pfoA-F	GCAAGTATTGCAATGGCTTT	Northern blotting
pfoA-R	GTAAGTAATACTAGATCCAGGGT	Northern blotting
colA-F	GGTCTAGAGGATAGTGGAAGA	Northern blotting
colA-R	GTTCCTCTCATATCGTAAGT	Northern blotting
0845-PE	TTTATCAATGGGTAACGTAAAGAAAGTACCAGATA	Primer extension
0846-PE	GTTGAAACTCCTCCTAATAGAACGCTACCAATGGT	Primer extension
0920-PE	TCGGTATAATAAAAATGATATTGTTACTAATATG	Primer extension
virT-NM	GAAAGTACCAGATTAAATAGAAATAG	Site-directed mutagenesis
virU-NM-1	TTGGTATTATATATTAATATTTTCGTC	Site-directed mutagenesis
virU-NM-2	GACGAAAATATTAATATATAATACCAA	Site-directed mutagenesis
virT-FM-F	ATCGCTTTAAGTTTATCATTTCTATTTTATCTGGT	Site-directed mutagenesis
virT-FM-R	ACCAGATAAAATAGAAATGATAAACTTAAAGCGAT	Site-directed mutagenesis
virU-FM-F	GATATGAAAGACGAAAAATTAATATAAAATACCAA	Site-directed mutagenesis
virU-FM-R	TTGGTATTTTATATTAATTTTTCGTCTTTCATATC	Site-directed mutagenesis

transcribed on opposite strands, these five genes are not clustered (Fig. 1). The deduced amino acid sequence of the putative protein encoded by *ccp* was highly similar to that of alpha-clostripain, a cysteine proteinase from *Clostridium histolyticum* (7). The expression of *ccp* was previously shown to be positively regulated by the VirR/VirS system (27). The putative proteins encoded by *virT* and *virU* showed no significant similarity to known proteins, and their functions remain unclear. Identification of the previously uncharacterized putative VirR-binding sites in *virT*, *ccp*, and *virU* led to an investigation of whether these three genes, like *pfoA* and *vrr*, are targets for direct regulation by the VirR/VirS system.

Transcriptional regulation of *virT*, *ccp*, and *virU* by the VirR/VirS system. We performed Northern analyses of RNA of *C. perfringens* strains with different mutant backgrounds at different growth stages to look for changes in the steady-state levels

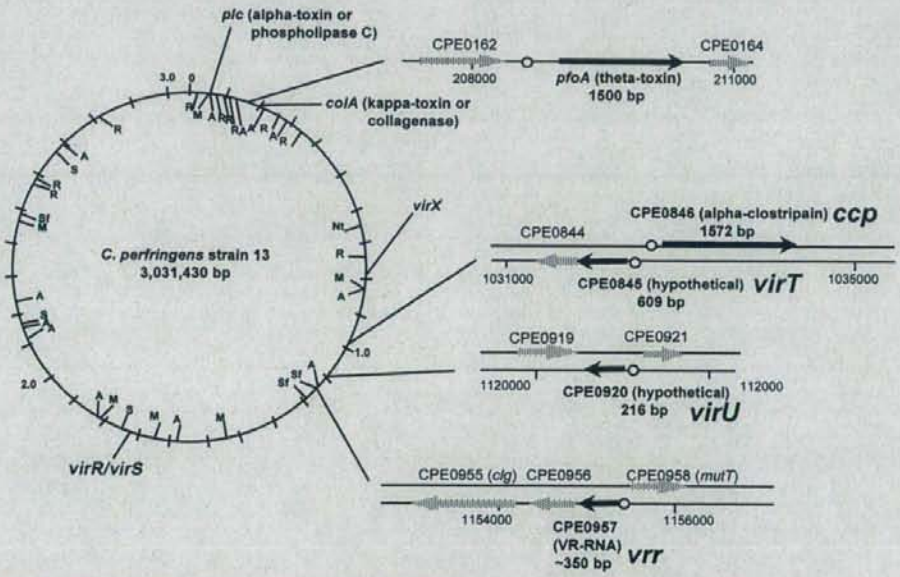

FIG. 1. Schematic diagram of the locations of putative VirR-binding sites in five genes (*pfoA*, *virT*, *ccp*, *virU*, and *vrr*) on the chromosome of *C. perfringens* wild-type strain 13. The solid and cross-hatched arrows represent genes with VirR-binding sites and their flanking genes, respectively. Open circles indicate putative VirR-binding sites. The chromosomal locations of other genes mentioned in this paper are also indicated. The nucleotide numbers are the numbers for the chromosomal sequence of *C. perfringens* strain 13 (GenBank accession number BA000016).

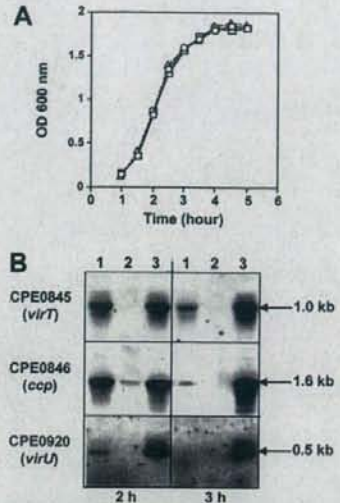

FIG. 2. Growth curves and Northern blot analyses for the *virR* mutant (TS133) of *C. perfringens*. (A) Growth curves for *C. perfringens* strains with a 1% inoculum. All three *C. perfringens* strains grew with a doubling time of ~20 min in Gifu anaerobic medium. ○, strain 13(pJIR418); □, strain TS133(pJIR418) (*virR*); △, strain TS133 (pBT405) (*virR*$^+$ *virS*$^+$). OD 600 nm, optical density at 600 nm. (B) Total RNA was prepared from each culture at the indicated times (2 and 3 h). Either 10 μg (for *virT* and *ccp*) or 40 μg (for *virU*) of total RNA was resolved by agarose electrophoresis, blotted onto a nylon membrane, and hybridized with probes for *virT* (CPE0845), *ccp* (CPE0846), and *virU* (CPE0920). Lane 1, strain 13(pJIR418); lane 2, strain TS133 (pJIR418); lane 3, strain TS133(pBT405).

of *virT*, *ccp*, and *virU* that confirmed that that there is regulation by the VirR/VirS system. In *C. perfringens* wild-type strain 13, a 1.0-kb transcript of *virT* was clearly detected after 2 h of growth (early to mid-exponential phase) (Fig. 2B, upper left panel), and the level had decreased after 3 h of incubation (late exponential phase) (Fig. 2B, upper right panel). Similar patterns were observed for expression of the 1.6-kb alpha-clostripain (*ccp*) transcript (Fig. 2B, center panels) and the 0.5-kb *virU* transcript (Fig. 2B, lower panels) in the wild-type background. Even with 40 μg of total RNA blotted onto the membrane, the *virU* transcript signal was very low for strain 13, indicating that the level of expression of *virU* was significantly lower than the level of expression of *virT* or *ccp*. The time points of accumulation for *virT*, *ccp*, and *virU* mRNAs were similar to those for *pfoA* and *vrr*; all of the molecules were most abundant during the early exponential to mid-exponential growth phase (3, 4). Importantly, transcripts of *virT*, *ccp*, and *virU* either were undetectable or the bands were very weak for the *virR* mutant strain TS133 (Fig. 2B, lane 2). Expression of these genes was increased by transformation of intact *virR* and *virS* genes into TS133 (Fig. 2B, lane 3). These data clearly indicate that the steady-state RNA levels for *virT*, *ccp*, and *virU* were regulated positively by the VirR/VirS system in *C. perfringens* in a manner similar to the manner of regulation of *pfoA* and *vrr* (3, 4, 28). The higher levels of the *virT*, *ccp*, and *virU* transcripts in the complemented strains were likely due to the high copy number of the pBT405 complementation plasmid.

Promoter analysis of the VirR/VirS-regulated genes. To analyze the promoter regions of the three VirR/VirS-regulated genes, we identified transcription initiation sites for *virT*, *ccp*, and *virU* by performing a primer extension experiment with wild-type and *virR* mutant RNA templates. The *virT*-specific primer generated a single extension product with wild-type strain 13 RNA, whereas no product was obtained with the *virR* mutant strain TS133 (Fig. 3A, left panel). Similarly, both the *ccp* and *virU* gene-specific primers (Fig. 3A, middle and right panels, respectively) yielded single extension products with the wild-type RNA template, whereas no products were obtained with *virR* mutant strain RNA. These results indicate that transcription initiation from single sites in *virT*, *ccp*, and *virU* is dependent on the VirR/VirS system because little mRNA for these genes was present in the *virR* mutant strain.

The length of each primer extension product was used to assign the position 1 site of transcription initiation for *virT*, *ccp*, and *virU* and to identify conserved elements (−35 and −10) in the promoter of each gene (Fig. 3B). We compared the locations of the VirR-binding sequences (CCAGTTWTNCA), the consensus promoter sequences (−35 and −10), and the mRNA start sites with those determined for *pfoA* and *vrr* in previous studies (4, 28) (Fig. 3B) and found that the relative distances between these elements were highly conserved in the five promoter regions. In particular, all five genes have a 42-bp interval between the VirR-binding sequences and the mRNA start site (Fig. 3B). The locations of the consensus promoter sequences (−35 and −10) were almost identical in all five genes.

In previous studies, two repeated sequences (VB1 and VB2) in the promoter region of *pfoA* (Fig. 3B) were identified as independent binding sites for the VirR protein (5, 6). The promoter regions of *vrr*, *virT*, *ccp*, and *virU* contained sequences similar to the VB2 sequence of *pfoA* (Fig. 3B). Although more divergent than the similarities between these four genes and *pfoA* in the VB2 consensus sequence, sequences similar to VB1 were found in these four genes (Fig. 3B), suggesting that the VB1 region may also be important for regulation of transcript by the VirR protein. The promoter structures of these five VirR-regulated genes are highly conserved and are distinct from the promoter structures of previously analyzed VirR/VirS-regulated genes (4, 19). The ability of the VirR protein to bind to the conserved sequences upstream of *virT*, *ccp*, and *virU* was confirmed in a previous study (5). Moreover, VirR has been reported to bind to some VirR boxes found in genes of two other strains of *C. perfringens*, ATCC13124 and SM101 (16), which suggests that the VirR-dependent regulatory system is present in various types of *C. perfringens* strains. Binding of a glutathione *S*-transferase–VirR fusion protein to the VirR-binding sequence was also examined using gel mobility shift assays, and this analysis confirmed that the VirR protein bound specifically to the conserved sequences in the promoter regions of *pfoA*, *vrr*, *virT*, *ccp*, and *virU* (data not shown).

Functional analysis of the *virT* and *virU* genes. We were unable to predict the putative function of either *virT* or *virU* using the results of computer-based searches for sequence similarities. To explore the functional roles of these genes, we

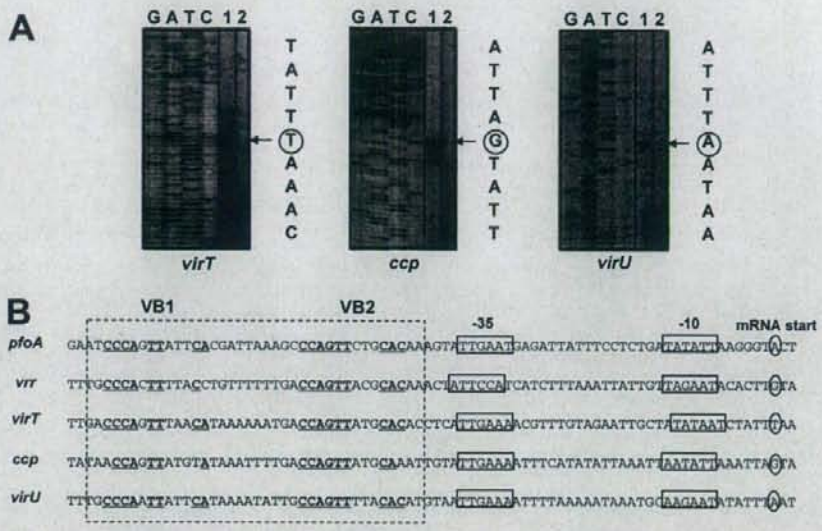

FIG. 3. Identification of the transcription initiation sites of the *virT*, *ccp*, and *virU* genes in *C. perfringens*. (A) Primer extension products derived using the oligonucleotide primers listed in Table 2 with template RNA prepared from 2-h cultures of *C. perfringens* strains (lane 1, wild-type strain 13; lane 2, *virR* strain TS133) were separated by electrophoresis on acrylamide gels. Sequencing reactions with the same primers and appropriate DNA templates were run on the same gel. The positions of extended products obtained with the *virT*, *ccp*, and *virU* primers are indicated by arrows, and the putative mRNA start sites are indicated by circles. (B) Deduced promoter sequences (−35 and −10) and consensus VirR-binding sites of the five VirR/VirS-regulated genes. The putative promoter sequences and mRNA start sites are indicated by boxes and circles, respectively. The deduced VirR-binding sequence of each gene is indicated by a dotted box, and conserved nucleotides are underlined. The promoter sequences of the theta-toxin (*pfoA*) and VR-RNA (*vrr*) genes are aligned, and the VB1 and VB2 regions are shown.

constructed *virT* isogenic mutants of strain 13 (see Materials and Methods). The resulting *virT* mutation in strain TS190, which was confirmed by Southern hybridization with a *virT* gene probe (data not shown), was used to examine expression of VirR/VirS-regulated genes. Compared to wild-type strain 13, in mutant strain TS190 there were at least 2.5-fold increases in the levels of both *pfoA* and *ccp* mRNAs during the logarithmic growth phase (2 and 3 h) (Fig. 4A). When mutant strain TS190 was complemented with the *virT*$^+$ pTS930 plasmid [resulting in TS190(pTS930)], the level of each of the transcripts was reduced to the wild-type level, although complementation was not complete until the 3-h time point for unknown reasons (Fig. 4A). These data suggest that the *virT* gene product acts as a negative regulator of *pfoA* and *ccp* in the wild-type strain. However, no significant change in *plc*, *colA*, *vrr*, or *virU* expression was observed in TS190 (Fig. 4A), indicating that the negative effect of the *virT* gene product was specific to *pfoA* and *ccp*.

For unknown reasons, repeated attempts to construct a strain 13 *virU* mutant using single-crossover or double-crossover recombination methods failed. As an alternative approach to test the function of *virU*, we introduced a *virU* overexpression plasmid, pTS931, into wild-type strain 13 to measure the effect of *virU* on the steady-state levels of putative VirR/VirS target genes. In 3-h cultures, the *pfoA*, *ccp*, *vrr*, and *virT* mRNA levels were all increased in response to the higher number of *virU* copies (Fig. 4B), suggesting that the *virU* gene encodes a positive regulator of *pfoA*, *ccp*, *vrr*, and *virT* expression. Although the abundance of *plc* and *colA* transcripts also increased slightly following transformation of pTS931 into strain 13 (Fig. 4B), we believe that this may have been a secondary effect of increased VR-RNA (Fig. 4B, *vrr* panels), which is known to enhance expression of *plc* and *colA*.

In addition to measuring changes in the levels of the *pfoA* and *ccp* mRNAs, we also measured the activities of the secreted gene products, perfringolysin O and alpha-clostripain, respectively, in supernatants from cultures of wild-type and mutant *C. perfringens* strains. Perfringolysin O activity was measured by determining the hemolytic activities of the culture supernatants with horse erythrocytes. The hemolytic activities of *virT* mutant strain TS190, TS190 with the plasmid expressing *virT* (pTS930), and wild-type strain 13 with the *virU* overexpression plasmid (pTS931) were 3.9-, 1.2- and 4.3-fold higher, respectively, than the hemolytic activity of wild-type strain 13 (Table 3). These results, which correspond well with the results of the Northern analyses, indicate that the activity encoded by wild-type *virU* stimulates the production of perfringolysin O, whereas the wild-type *virT* gene product inhibits the production of perfringolysin O.

Azocasein, a colorimetric substrate of alpha-clostripain and other cysteine proteinases, was used to measure alpha-clostripain activity specifically in culture supernatants containing two inhibitors of cysteine proteinases, leupeptin and antipain. In the presence of these inhibitors, the proteolytic activity of each strain, as measured by absorbance at 450 nm, decreased between 25 and 60% (Fig. 5A). The difference in activity represents alpha-clostripain-specific proteolysis of azocasein (Fig. 5B). The alpha-clostripain activity was increased in the *virT* mutant strain TS190, and when the mutation was complemented with pTS930 (*virT*$^+$), the activity decreased to a level

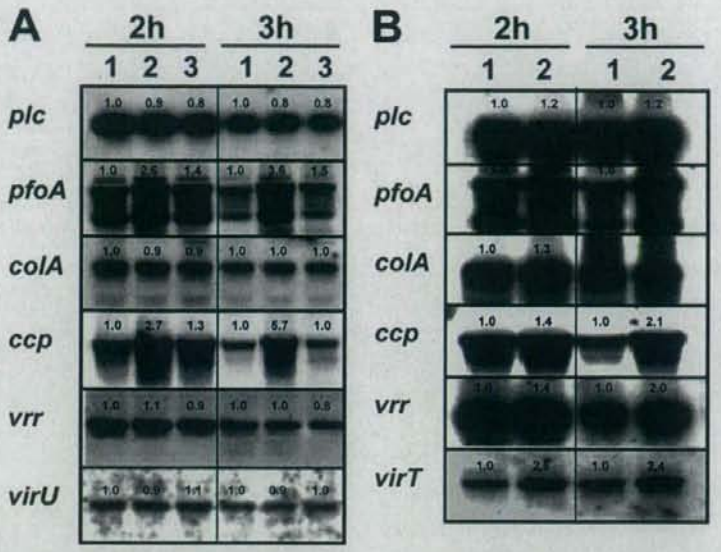

FIG. 4. Northern blot analyses of the *virT* mutant and wild-type strains transformed with the *virU*$^+$ expression plasmid (pTS931). Total RNA was prepared from each culture at the times indicated (2 and 3 h), and 10 μg of each RNA preparation (40 μg for hybridization with *virU* probe) was resolved by agarose electrophoresis, blotted onto nylon membranes, and hybridized with *plc*, *pfoA*, *colA*, *ccp*, *vrr*, *virT*, and *virU* gene probes as indicated. The band densities relative to those for wild-type strain 13 are indicated above the bands. (A) Lane 1, wild-type strain 13(pJIR418); lane 2, strain TS190(pJIR418) (Δ*virT*); lane 3, strain TS190(pTS930) (Δ*virT virT*$^+$). (B) Lane 1, wild-type strain 13(pJIR418); lane 2, wild-type strain 13(pTS931) (*virU*$^+$).

similar to the level in the wild-type strain (Fig. 5B), indicating that expression of alpha-clostripain is negatively regulated by *virT*. Similarly, the alpha-clostripain activity was higher in the *virU*-overexpressing strain than in the wild-type strain (Fig. 5B), suggesting that the *virU* gene product stimulates alpha-clostripain production. The similarities between the changes in perfringolysin O and alpha-clostripain activities and the changes in the levels of mRNAs for these genes in different genetic backgrounds (wild-type strain versus *virT* mutant or *virU*-overexpressing strain) suggest that the *virT* gene product negatively controls expression of *pfoA* and *ccp* and that the *virU* gene product enhances expression of *pfoA* and *ccp* in *C. perfringens*.

Mutational analyses of *virT* and *virU*. It has been reported that in *C. perfringens* regulatory RNA molecules control expression of several genes, including toxin genes (17, 28). Con-

TABLE 3. Perfringolysin O activities of various *C. perfringens* strains

Strain	Genotype	Perfringolysin O titer (log_2)[a]	Difference (fold) compared to strain 13
13	Wild type	7.4 ± 0.5	1
TS133	Strain 13 *virR*::Tet^r	2.0 ± 0.1	<0.1
TS190	Strain 13 Δ*virT*	9.4 ± 0.5	3.9
TS190(pTS930)	Strain 13 Δ*virT* (*virT*$^+$)	7.7 ± 0.4	1.2
13(pTS931)	Strain 13 (*virU*$^+$)	9.5 ± 0.7	4.3

[a] Each value was calculated by using the results of triplicate independent experiments, and the values are means ± standard deviations.

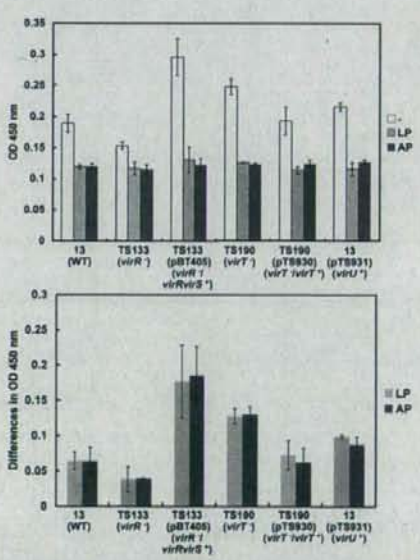

FIG. 5. Alpha-clostripain activities of various *C. perfringens* strains. (A) The alpha-clostripain activity of each *C. perfringens* strain (indicated at the bottom) was determined with azocasein as a substrate under conditions with no inhibitor (−), with leupeptin (LP), or with antipain (AP). For each strain and treatment combination, the mean absorbance and standard deviation (error bar) calculated from three independent experiments are shown. (B) The difference in mean proteolytic activity between assays without inhibitors and assays with the leupeptin or antipain inhibitor (shown in panel A), which represents alpha-clostripain-specific proteolytic activity, was plotted for each *C. perfringens* strain. WT, wild type; OD 450 nm, optical density at 450 nm.

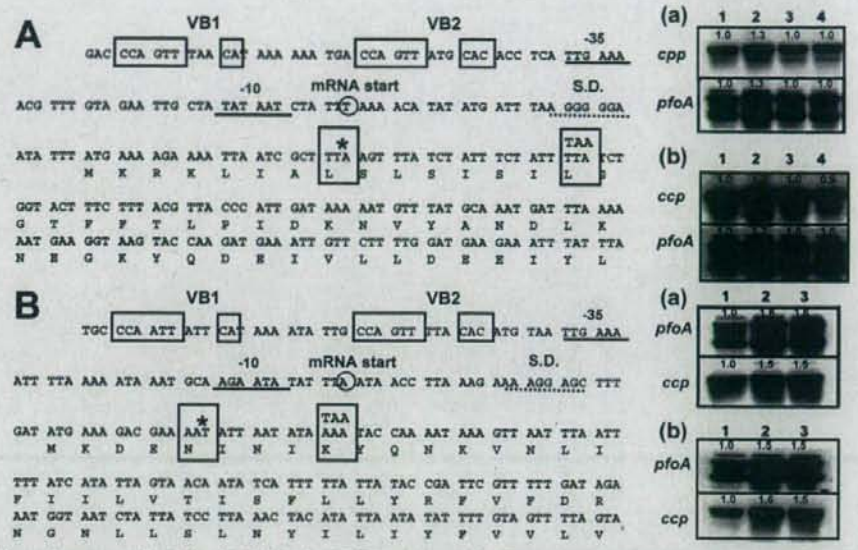

FIG. 6. Site-directed mutagenesis of the *virT* (A) and *virU* (B) genes and the effects of the mutations on steady-state levels of VirR-regulated gene mRNAs. The nonsense and frameshift codons engineered in the *virT* and *virU* coding regions (left panels) are indicated by large boxes. The positions of the nonsense mutation (NM) and frameshift mutation (FM) are indicated by TAA and an asterisk, respectively. Plasmids carrying mutated *virT* and *virU* genes (designated pTS932 and pTS935 for *virT* and pTS933 and pTS935 for *virU*) were transformed into different *C. perfringens* strains. The band densities relative to those for wild-type strain 13 are indicated above the bands. (A) (Panel a) Lane 1, wild-type strain 13(pJIR418); lane 2, strain TS190(pJIR418) (Δ*virT*); lane 3, strain TS190(pTS930 (Δ*virT virT*$^{+}$); lane 4, strain TS190(pTS932) (Δ*virT virT*^{NM}). (Panel b) Lane 1, wild-type strain 13(pJIR418); lane 2, strain TS190(pJIR418) (Δ*virT*); lane 3, strain TS190(pTS930) (Δ*virT virT*$^{+}$); lane 4, strain TS190(pTS935) (Δ*virT virT*^{FM}). (B) (Panel a) Lane 1, wild-type strain 13(pJIR418); lane 2, wild-type strain 13(pTS931) (*virU*$^{+}$); lane 3, wild-type strain 13(pTS933) (*virU*^{NM}). (Panel b) Lane 1, wild-type strain 13(pJIR418); lane 2, wild-type strain 13(pTS931) (*virU*$^{+}$); lane 3, wild-type strain 13(pTS9360 (*virU*^{FM}). Northern analyses were performed with the indicated probes (right panels).

sidering the relatively small size of the *virT* and *virU* ORFs (609 and 216 bp, respectively), it is possible that these genes, like *vrr* and *virX*, encode regulatory RNAs. To test this hypothesis, nonsense mutations were introduced into the protein-encoding regions of *virT* and *virU* with plasmid vectors (pTS932 and pTS933, respectively), and then differences between the *ccp* and *pfoA* steady-state mRNA levels in samples of wild-type and mutant cell total RNAs were determined (Fig. 6). When the *virT* nonsense mutant gene in pTS932 was introduced into the isogenic *virT* mutant strain TS190, the relative levels of *ccp* and *pfoA* transcripts in TS190(pTS932) were not different from the levels in TS190(pTS930) containing an intact *virT* gene (Fig. 6A, panel a, lanes 3 and 4). Similarly, a nonsense mutation was constructed in the coding region of *virU* in plasmid pTS933, which was transformed into wild-type strain 13 (Fig. 6B). The results indicated that there was a difference in the level of *vrr*, *pfoA*, or *ccp* mRNA between wild-type strain 13 overexpressing intact *virU* (pTS931) and wild-type strain 13 overexpressing mutated *virU* (pTS933) (Fig. 6B, panel a, lanes 2 and 3). Furthermore, one-base deletions at positions 33 and 15 in the *virT* and *virU* coding regions (Fig. 6) were introduced to generate frameshift mutations, resulting in plasmids pTS935 and pTS936, respectively. Plasmid pTS935 was transformed into the isogenic *virT* mutant strain TS190 and wild-type strain 13, and the mRNA levels for *pfoA* and *ccp* were determined by Northern hybridization. As shown in Fig. 6, the relative levels of *ccp* and *pfoA* transcripts in TS190(pTS935) with frameshifted *virT* were not different from the levels in TS190 (pTS930) containing an intact *virT* gene. Similarly, the transcript levels of *ccp* and *pfoA* were not different in strain 13 harboring pTS936 (with frameshifted *virU*) and strain 13 harboring pTS931. Taken together, these results indicate that there was no difference in the regulatory functions of *virT* and *virU* whether the ORFs were intact or not intact. These data strongly suggest that both the *virT* and *virU* genes encode regulatory RNA molecules, not proteins, that regulate the VirR/VirS regulon. The promoters of *pfoA*, *virT*, *ccp*, *vrr*, and *virU* were screened, and no conserved sequence motifs (besides the VirR consensus sequence) were found, indicating that it is unlikely that there are other regulatory RNAs or proteins that are shared by these VirR/VirS-regulated genes.

DISCUSSION

A genome-wide search for promoter-proximal VirR-binding sites previously identified the theta-toxin-encoding gene *pfoA* (6) and the *vrr* gene, which encodes regulatory VR-RNA (28), and also identified three new genes, *virT*, *ccp*, and *virU*, as potential members of the VirR/VirS regulon (25). To test the veracity of this in silico identification, genetic and molecular analyses of *virT*, *ccp*, and *virU* functions and regulation by the VirR/VirS system were performed.

Comparative Northern analyses of wild-type and *virR* mutant strains of *C. perfringens* revealed that *virT*, *ccp*, and *virU*

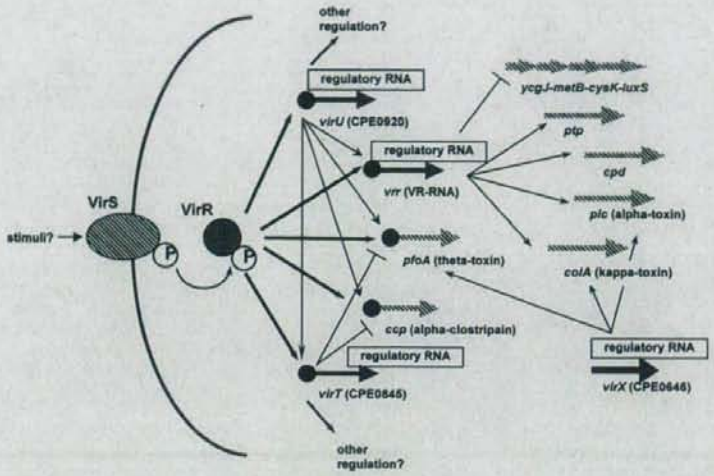

FIG. 7. Schematic diagram of the VirR/VirS regulon. The diagram was constructed by using the results of this and previous studies (3, 4, 12, 17, 18, 20, 24, 25, 28).

are positively regulated by the VirR/VirS system at the RNA level. The sequence and location of a putative VirR-binding consensus site (VB1/VB2) and its location (from position −40 to position −80 upstream of the initiation site) were conserved in the *pfoA*, *vrr*, *virT*, *ccp*, and *virU* promoters, suggesting that VirR may bind directly to these sites to activate transcription (5). Gel shift assays confirmed that the VirR protein binds specifically to the conserved promoter sequences. These data led us to conclude that the VirR/VirS regulon involves five genes regulated directly by the VirR protein in *C. perfringens* (Fig. 7).

The deduced amino acid sequence encoded by *ccp* is highly similar to the amino acid sequence of alpha-clostripain from *C. histolyticum* (EC 3.4.22.8) (7), which is a heterodimeric cysteine endopeptidase with specificity for Arg-X peptidyl bonds (7, 8). The two polypeptide chains (termed light and heavy) of the native enzyme are encoded by a single 1,581-bp gene, and the junction between the two polypeptide DNA sequences encodes a linker nonapeptide (7). Alpha-clostripain has been implicated in damage of cells in fetal rat calvaria (10) and may contribute to the virulence of other clostridial infections (23). Detection of alpha-clostripain protein and the enzymatic activity in the supernatants of *C. perfringens* cultures (27) suggest that alpha-clostripain may be a virulence factor. The *C. perfringens* genome lacks many genes needed for amino acid biosynthesis, and alpha-clostripain may participate in degradation of host proteins that yields nutrients required for *C. perfringens* survival and growth (25). Further studies are needed to elucidate the roles of alpha-clostripain in *C. perfringens* nutrient uptake and pathogenicity.

Although we were unable to predict the functions of the molecules encoded by *virT* and *virU* based on homology with other genes (25), the activities of these molecules clearly influence VirR/VirS gene regulation; the *virT* product acts as a negative regulator of expression, and the *virU* product acts as a positive regulator of expression (Fig. 4). The inability to alter these effects by nonsense mutations in *virT* and *virU* suggests that these genes, like *vrr* (28) and *virX* (17), encode regulatory RNA molecules rather than proteins (Fig. 6). A possible secondary structure was examined for the predicted *virT* and *virU* RNA molecules. The predicted secondary structures of the whole *virT* and *virU* RNAs were tight and compact overall, similar to the structure predicted for VR-RNA (data not shown) (28). The transcriptional terminator downstream of the *virT* and *virU* regions was also searched, and only *virU* was found to have inverted repeat sequences. Furthermore, Northern analyses were performed with 50-mer synthetic sense and antisense oligonucleotide probes to look for changes in the steady-state levels of *virT* and *virU* mRNAs. Both *virT* and *virU* transcripts were detected in wild-type strain 13 with antisense probes, whereas no signals were obtained with the sense *virT* and *virU* probes (data not shown).

Unexpectedly, the number of regulatory RNA molecules found to be involved in regulation of virulence (and other) genes in *C. perfringens* is increasing. Based on recent reports of the importance of small RNA molecules in regulation of transcription and/or translation in both prokaryotes and eukaryotes (12, 15), many RNA molecules involved in other aspects of *C. perfringens* gene regulation may still be unknown. In the case of the *virT* and *virU* RNAs, the absence of a putative consensus sequence for direct annealing of these RNAs to the promoters of the *virT*- and *virU*-regulated genes *pfoA*, *virT*, *ccp*, *virU*, and *vrr* suggests that these regulatory RNAs may affect the activity of other proteins or RNA regulators for these five genes. Because the effects of *virT* and *virU* mutations on transcription were much more subtle than those of the VirR/VirS system or VR-RNA, *virT* and *virU* may fine-tune transcription of VirR/VirS-regulated genes to maintain balanced gene expression. Future studies of the effects of *virT* and *virU* on gene regulation, such as DNA microarray analyses of *C. perfringens* cultured under changing environmental con-

ditions, may provide a more detailed view of the overall effects of these regulatory genes.

The conclusion that the VirR/VirS system directly regulates only five genes (*pfoA*, *vrr*, *virT*, *ccp*, and *virU*) in *C. perfringens* via VirR binding is somewhat surprising. It has been reported that the VirR/VirS system influences expression of many other genes, including *plc* (encoding alpha-toxin), *colA* (encoding kappa-toxin), *cpd* (encoding 2′,3′-cyclic nucleotide phosphodiesterase), *ptp* (encoding protein tyrosine phosphatase), *ycgJ* (encoding a hypothetical protein), *metB* (encoding cystathionine gamma-lyase), *cysK* (encoding cysteine synthase), and *luxS* (encoding the autoinducer 2 production protein) (3, 4, 18, 20). However, for *plc*, *colA*, *cpd*, *ptp*, and *ycgJ-metB-cysK-luxS*, VR-RNA has been shown to be a secondary RNA regulator (3, 28) (Fig. 7). Another RNA regulator, *virX*, controls the levels of *pfoA*, *plc*, and *colA* mRNAs independent of the VirR/VirS regulatory cascade (17) (Fig. 7). Furthermore, cell-cell signaling by autoinducer 2 synthesized by the *luxS* gene product, which may be mediated through an unidentified two-component system (18), also plays an important role in the regulation of toxin production.

It is clear that the VirR/VirS regulon consists of two classes of genes, the genes that are regulated directly by the VirR/VirS system and the genes that are regulated indirectly (Fig. 7). The mechanism of regulation of the VirR/VirS regulon, including the actions of the *virT* and *virU* regulatory RNA molecules, should be clarified by comprehensive DNA microarray-based analyses of gene expression.

ACKNOWLEDGMENTS

We thank Harumi Yaguchi for supplying the *vrr* mutant strain and Kaori Honjo, Yukari Tajima, and Hameem I. Kawsar for helpful discussions.

This work was supported by the Research for the Future Program of the Japan Society for the Promotion of Science, by Grants-in Aid for Scientific Research (B) from the Japan Society for the Promotion of Science, and by KAKENHI (Grant-in-Aid for Scientific Research on Priority Areas "Applied Genomics") from the Ministry of Education, Culture, Sports, Science and Technology of Japan.

REFERENCES

1. **Aiba, H., S. Adhya, and B. de Crombrugghe.** 1981. Evidence for two functional gal promoters in intact *Escherichia coli* cells. J. Biol. Chem. **256:**11905–11910.
2. **Awad, M. M., A. E. Bryant, D. L. Stevens, and J. I. Rood.** 1995. Virulence studies on chromosomal alpha-toxin and theta-toxin mutants constructed by allelic exchange provide genetic evidence for the essential role of alpha-toxin in *Clostridium perfringens*-mediated gas gangrene. Mol. Microbiol. **15:**191–202.
3. **Banu, S., K. Ohtani, H. Yaguchi, T. Swe, S. T. Cole, H. Hayashi, and T. Shimizu.** 2000. Identification of novel VirR/VirS-regulated genes in *Clostridium perfringens*. Mol. Microbiol. **35:**854–864.
4. **Ba-Thein, W., M. Lyristis, K. Ohtani, I. T. Nisbet, H. Hayashi, J. I. Rood, and T. Shimizu.** 1996. The *virR/virS* locus regulates the transcription of genes encoding extracellular toxin production in *Clostridium perfringens*. J. Bacteriol. **178:**2514–2520.
5. **Cheung, J. K., B. Dupuy, D. S. Deveson, and J. I. Rood.** 2004. The spatial organization of the VirR boxes is critical for VirR-mediated expression of the perfringolysin O gene, *pfoA*, from *Clostridium perfringens*. J. Bacteriol. **186:**3321–3330.
6. **Cheung, J. K., and J. I. Rood.** 2000. The VirR response regulator from *Clostridium perfringens* binds independently to two imperfect direct repeats located upstream of the *pfoA* promoter. J. Bacteriol. **182:**57–66.
7. **Dargatz, H., T. Diefenthal, V. Witte, G. Reipen, and D. von Wettstein.** 1993. The heterodimeric protease clostripain from *Clostridium histolyticum* is encoded by a single gene. Mol. Gen. Genet. **240:**140–145.
8. **Gilles, A. M., J. M. Imhoff, and B. Keil.** 1979. Alpha-clostripain. Chemical characterization, activity, and thiol content of the highly active form of clostripain. J. Biol. Chem. **254:**1462–1468.
9. **Hatheway, C. L.** 1990. Toxigenic clostridia. Clin. Microbiol. Rev. **3:**66–98.
10. **Hefley, T., J. Cushing, and J. S. Brand.** 1981. Enzymatic isolation of cells from bone: cytotoxic enzymes of bacterial collagenase. Am. J. Physiol. **240:**C234–C238.
11. **Janoir, C., S. Péchiné, C. Grosdidier, and A. Collignon.** 2007. Cwp84, a surface-associated protein of *Clostridium difficile*, is a cystein protease with degrading activity on extracellular matrix proteins. J. Bacteriol. **189:**7174–7180.
12. **Johansson, J., and P. Cossart.** 2003. RNA-mediated control of virulence gene expression in bacterial pathogens. Trends Microbiol. **11:**280–285.
13. **Lyristis, M., A. E. Bryant, J. Sloan, M. M. Awad, I. T. Nisbet, D. L. Stevens, and J. I. Rood.** 1994. Identification and molecular analysis of a locus that regulates extracellular toxin production in *Clostridium perfringens*. Mol. Microbiol. **12:**761–777.
14. **Mahony, D. E., and T. I. Moore.** 1976. Stable L-forms of *Clostridium perfringens* and their growth on glass surfaces. Can. J. Microbiol. **22:**953–959.
15. **Masse, E., N. Majdalani, and S. Gottesman.** 2003. Regulatory roles for small RNAs in bacteria. Curr. Opin. Microbiol. **6:**120–124.
16. **Myers, G. S. A., D. A. Rasko, J. K. Cheung, J. Ravel, R. Seshadri, R. T. DeBoy, Q. Ren, J. Varga, M. M. Awad, L. M. Brinkac, S. C. Daugherty, D. H. Haft, R. J. Dodson, R. Madupu, W. C. Nelson, M. J. Rosovitz, S. A. Sullivan, H. Khouri, G. I. Dimitrov, K. L. Watkins, S. Mulligan, J. Benton, D. Radune, D. J. Fisher, H. S. Atkins, T. Hiscox, B. H. Jost, S. J. Billington, J. G. Songer, B. A. McClane, R. W. Titball, J. I. Rood, S. B. Melville, and I. T. Paulsen.** 2006. Skewed genomic variability in strains of the toxigenic bacterial pathogen, Clostridium perfringens. Genome Res. **16:**1031–1040.
17. **Ohtani, K., S. K. Bhowmik, H. Hayashi, and T. Shimizu.** 2002. Identification of a novel locus that regulates expression of toxin genes in *Clostridium perfringens*. FEMS Microbiol. Lett. **209:**113–118.
18. **Ohtani, K., H. Hayashi, and T. Shimizu.** 2002. The *luxS* gene is involved in cell-cell signaling for toxin production in *Clostridium perfringens*. Mol. Microbiol. **44:**171–179.
19. **Ohtani, K., H. I. Kawsar, K. Okumura, H. Hayashi, and T. Shimizu.** 2003. The VirR/VirS regulatory cascade affects transcription of plasmid-encoded putative virulence genes in *Clostridium perfringens*. FEMS Microbiol. Lett. **222:**137–141.
20. **Ohtani, K., H. Takamura, H. Yaguchi, H. Hayashi, and T. Shimizu.** 2000. Genetic analysis of the *ycgJ-metB-cysK-ygaG* operon negatively regulated by the VirR/VirS system in *Clostridium perfringens*. Microbiol. Immunol. **44:**525–528.
21. **Petit, L., M. Gibert, and M. R. Popoff.** 1999. *Clostridium perfringens*: toxinotype and genotype. Trends Microbiol. **7:**104–110.
22. **Sambrook, J., E. F. Fritch, and T. Maniatis.** 1989. Molecular cloning: a laboratory manual, 2nd ed. Cold Spring Harbor Laboratory, Cold Spring Harbor, NY.
23. **Seddon, S. V., and S. P. Borriello.** 1992. Proteolytic activity of *Clostridium difficile*. J. Med. Microbiol. **36:**307–311.
24. **Shimizu, T., W. Ba-Thein, M. Tamaki, and H. Hayashi.** 1994. The *virR* gene, a member of a class of two-component response regulators, regulates the production of the perfringolysin O, collagenase, and hemagglutinin in *Clostridium perfringens*. J. Bacteriol. **176:**1616–1623.
25. **Shimizu, T., K. Ohtani, H. Hirakawa, K. Ohshima, A. Yamashita, T. Shiba, N. Ogasawara, M. Hattori, S. Kuhara, and H. Hayashi.** 2002. Complete genome sequence of *Clostridium perfringens*, an anaerobic flesh-eater. Proc. Natl. Acad. Sci. USA **99:**996–1001.
26. **Shimizu, T., A. Okabe, and J. I. Rood.** 1997. Regulation of toxin production in *Clostridium perfringens*, p. 451–470. *In* J. I. Rood, G. Songer, B. A. McClane, and R. W. Titball (ed.), The clostridia: molecular biology and pathogenesis. Academic Press, London, United Kingdom.
27. **Shimizu, T., K. Shima, K. Yoshino, K. Yonezawa, T. Shimizu, and H. Hayashi.** 2002. Proteome and transcriptome analysis of the virulence genes regulated by the VirR/VirS system in *Clostridium perfringens*. J. Bacteriol. **184:**2587–2594.
28. **Shimizu, T., H. Yaguchi, K. Ohtani, S. Banu, and H. Hayashi.** 2002. Clostridial VirR/VirS regulon involves a regulatory RNA molecule for expression of toxins. Mol. Microbiol. **43:**257–265.
29. **Sloan, J., T. A. Warner, P. T. Scott, T. L. Bannam, D. I. Berryman, and J. I. Rood.** 1992. Construction of a sequenced *Clostridium perfringens-Escherichia coli* shuttle plasmid. Plasmid **27:**207–219.

JOURNAL OF BACTERIOLOGY, Jan. 2008, p. 48–60 Vol. 190, No. 1
0021-9193/08/$08.00+0 doi:10.1128/JB.01407-07

Carbon Catabolite Repression of Type IV Pilus-Dependent Gliding Motility in the Anaerobic Pathogen *Clostridium perfringens*▽†

Marcelo Mendez,[1]‡ I-Hsiu Huang,[2,3]‡ Kaori Ohtani,[4] Roberto Grau,[1]* Tohru Shimizu,[4] and Mahfuzur R. Sarker[2,3]

Instituto de Biología Molecular y Celular de Rosario (IBR-CONICET), Departamento de Microbiología, Facultad de Ciencias Bioquímicas y Farmacéuticas, Universidad Nacional de Rosario, Argentina[1]; Department of Biomedical Sciences, College of Veterinary Medicine, Oregon State University, Corvallis, Oregon[2]; Department of Microbiology, College of Science, Oregon State University, Corvallis, Oregon[3]; and Department of Bacteriology, Kanazawa University, Kanazawa, Japan[4]

Received 29 August 2007/Accepted 23 October 2007

***Clostridium perfringens* is an anaerobic, gram-positive, spore-forming bacterium responsible for the production of severe histotoxic and gastrointestinal diseases in humans and animals. In silico analysis of the three available genome-sequenced *C. perfringens* strains (13, SM101, and ATCC13124) revealed that genes that encode flagellar proteins and genes involved in chemotaxis are absent. However, those strains exhibit type IV pilus (TFP)-dependent gliding motility. Since carbon catabolite regulation has been implicated in the control of different bacterial behaviors, we investigated the effects of glucose and other readily metabolized carbohydrates on *C. perfringens* gliding motility. Our results demonstrate that carbon catabolite regulation constitutes an important physiological regulatory mechanism that reduces the proficiencies of the gliding motilities of a large number of unrelated human- and animal-derived pathogenic *C. perfringens* strains. Glucose produces a strong dose-dependent inhibition of gliding development without affecting vegetative growth. Maximum gliding inhibition was observed at a glucose concentration (1%) previously reported to also inhibit other important behaviors in *C. perfringens*, such as spore development. The inhibition of gliding development in the presence of glucose was due, at least in part, to the repression of the genes *pilT* and *pilD*, whose products are essential for TFP-dependent gliding proficiency. The inhibitory effects of glucose on *pilT* and *pilD* expression were under the control of the key regulatory protein CcpA (catabolite control protein A). The deficiency in CcpA activity of a *ccpA* knockout *C. perfringens* mutant strain restored the expressions of *pilT* and *pilD* and gliding proficiency in the presence of 1% glucose. The carbon catabolite repression of the gliding motility of the *ccpA* mutant strain was restored after the introduction of a complementing plasmid harboring a wild-type copy of *ccpA*. These results point to a central role for CcpA in orchestrating the negative effect of carbon catabolite regulation on *C. perfringens* gliding motility. Furthermore, we discovered a novel positive role for CcpA in *pilT* and *pilD* expression and gliding proficiency in the absence of catabolite regulation. Carbon catabolite repression of gliding motility and the dual role of CcpA, either as repressor or as activator of gliding, are analyzed in the context of the different social behaviors and diseases produced by *C. perfringens*.**

Motility is an important attribute utilized by many pathogenic and nonpathogenic bacteria to colonize new environments, to search for nutrients, and to allow the formation of complex architectural structures (e.g., biofilms and fruiting bodies) (14, 15, 25). Translocation in liquid medium (swimming) is mediated by flagella, and the swimming model has been traditionally used to describe bacterial motility. However, it is also true that in nature, most bacteria are associated with surfaces and therefore have evolved diverse mechanisms of translocation on solid or semisolid biotic and abiotic surfaces which are important for rapid dissemination and colonization during the course of an infection (21). Among the surface-associated mechanisms of motility that play key roles in cell-cell and cell-surface interactions, it is worth mentioning (i) swarming, a flagellum-dependent social form of translocation where planktonic cells differentiate into giant and hyperflagellated cells that move in groups ("swarms") to explore and colonize new habitats (10); (ii) twitching, a flagellum-independent but type IV pilus (TFP)-dependent form of intermittent and jerky surface motility (4, 14, 15), which has been demonstrated to occur in the opportunistic pathogen *Pseudomonas aeruginosa* (5), in the pathogen *Neisseria gonorrhoeae* (23), and recently in *Haemophilus influenzae*, which was previously considered a nonmotile bacterium (2); and (iii) gliding, which has been studied in detail in model organisms, such as *Myxococcus xanthus* and *Synechocystis* and *Anabaena* spp. (19). In *M. xanthus*, two types of mechanisms for gliding motility are utilized: adventurous gliding and social gliding (16). Adventurous gliding motility is observed when cells are isolated or in low numbers without contact with each other. In this sense, gliding motility is defined as a smooth movement of rod-shaped cells in the direction of their long axes on a surface. It has been proposed that the driving force for adventurous gliding motility in *M. xanthus* is generated by the action of a nozzle-like struc-

* Corresponding author. Mailing address: IBR, Facultad de Bioquímica y Farmacia, Universidad Nacional de Rosario, Suipacha 531, Rosario 2000, Argentina. Phone: 54-341-4353377. Fax: 54-341-4804605. E-mail: robertograu@fulbrightweb.org.

† Supplemental material for this article may be found at http://jb.asm.org/.

‡ The first two authors contributed equally.

▽ Published ahead of print on 2 November 2007.

ture that produces a polysaccharide slime trail. Social gliding motility, similar to twitching motility, is dependent on the active extension and retraction of TFP (16). For other bacteria (e.g., *Cytophaga* spp., *Flavobacterium* spp., and *Mycoplasma mobile*), gliding takes place in the absence of TFP and ATP consumption. Instead, they generate motility with motility proteins anchored to the membrane that in turn use proton motive force and/or polar polysaccharide extrusion to achieve cellular motility over surfaces; all these gliding examples point out the extreme diversity of gliding mechanisms (4, 14, 15, 22, 24). Extracellular TFP appendages are polymers of the small protein PilA, or pilin. In *P. aeruginosa*, PilA is initially translated as a prepilin with a short leader peptide cleaved by PilD (48); PilB provides energy for assembly. PilT and PilU are nucleoside triphosphate binding proteins that have been implicated in pilus retraction during twitching motility (4). In *P. aeruginosa*, almost 40 genes are involved in the biosynthesis and function of TFP (23, 47). Besides the key role of TFP in twitching and gliding, these appendages also mediate other important phenomena, such as adherence, fruiting body formation, bacteriophage absorption, DNA uptake, cytotoxicity, activation of host cell responses, and biofilm development (1, 14, 23, 24, 31).

Clostridium perfringens is a gram-positive, anaerobic, spore-forming bacterium that causes severe gastrointestinal and histotoxic infections in humans and animals (28, 32, 33). This pathogen has been traditionally described as a nonmotile bacterium, as no genes that encode flagellar proteins or genes involved in chemotaxis were identified in the complete genomic sequences of the three human-pathogenic *C. perfringens* strains 13, SM101, and ATCC13124 (26, 36). However, sequence analysis (data not shown) suggests that the three strains carry genes which code for TFP components (such as *pilA* to *pilD* and *pilT*) (26, 36). Recently, Varga et al. demonstrated that *C. perfringens* strains 13, SM101, and ATCC13124 exhibited social gliding motility on brain heart infusion agar (BHIA) plates, and TFP were detected on the surfaces of the bacteria (41). This study also demonstrated that *pilT* and *pilC* mutants failed to produce detectable pili and were nonmotile on BHIA (41). Other putative TFP biosynthesis genes found in *C. perfringens* remain to be characterized, and the exact mechanism of TFP assembly and its physiological role, importance, and regulation are currently unknown.

In this respect, diverse bacterial behaviors, such as biofilm development, sporulation, fruiting body formation, and surface-associated motility, are regulated by environmental, metabolic, and quorum-sensing signals (9, 10, 16, 28, 46). In particular, carbon catabolite regulation is a widespread phenomenon in bacteria where the expressions of a number of genes are regulated by the presence of a preferred carbon source, such as glucose or fructose (27, 39, 43). In *C. perfringens*, and many low-G+C-content, gram-positive bacteria, carbon catabolite control is under the regulation of CcpA (catabolite control protein A), a pleiotropic transcriptional regulator belonging to the LacI/GalR family of transcription factors (27, 39, 43). CcpA functions as a DNA binding protein, either activating or repressing genes generally in the presence of a preferred carbon source (35, 43). More precisely, surface-associated motility is an interesting example of social bacterial behavior that could be regulated by nutrient (i.e., carbon) availability in nature. Interestingly, in *P. aeruginosa*, swarming (but not twitching) motility is carbon source regulated; poor swarming activity is observed in the presence of glucose (37). Therefore, the ability of the pathogen to carry out surface-associated social motility during the course of the infection is of crucial importance (2, 10, 14, 21, 24). In this work, we have investigated the effects of glucose and other readily metabolized carbohydrates on the TFP-dependent social gliding motilities of a collection of pathogenic *C. perfringens* strains isolated from human and animal sources. Our results clearly demonstrate that carbon catabolite repression is a general and common regulatory mechanism of gliding motility in *C. perfringens*, independent of the source of isolation (human or animal) or type of infection (diarrhea or myonecrosis). We demonstrate that the repressive effect of glucose on gliding motility is partially due to the CcpA-mediated down-regulation of TFP biosynthesis genes. In addition, we have discovered and analyzed a novel carbon catabolite-independent positive role for CcpA in *C. perfringens* gliding motility.

TABLE 1. *C. perfringens* strains and plasmids used in this study

Strain or plasmid	Isolation source or phenotype	Source or reference
C. perfringens strains		
Human isolates		
Strain 13	Gas gangrene	36
KO13	*ccpA* mutant derivative of strain 13	This study
NCTC8239	Food poisoning	7
NCTC10239	Food poisoning	7
SM101	Food poisoning	49
191-10	Food poisoning	38
F4406	Sporadic diarrhea	7
F4969	Sporadic diarrhea	7
F5603	Sporadic diarrhea	7
B11	Antibiotic-associated diarrhea	7
B41	Antibiotic-associated diarrhea	7
NB16	Antibiotic-associated diarrhea	7
Animal isolates		
JGS1807	Diarrheic pig	45
JGS1818	Diarrheic pig	45
294442	Diarrheic dog	R. Carman
317206	Diarrheic dog	R. Carman
AHT327	Diarrheic horse	44
AHT2911	Diarrheic horse	44
Plasmids		
pMRS127	*sigK-gusA* in pJIR751	30
pEJZ2	*pilT* promoter fused with *gusA* in pMRS127	This study
p*PilD*gus-127	*pilD* promoter fused with *gusA* in pMRS127	This study
KO2		This study
pJIR750	*C. perfringens-E. coli* shuttle vector	3
pIH100		This study

MATERIALS AND METHODS

Strains and culture conditions. The *C. perfringens* strains used in this study are listed in Table 1. The growth media employed to propagate strains were fluid thioglycolate (FTG) and TGY (3% tryptic soy broth, 2% glucose, 1% yeast extract, and 0.1% cysteine) (8, 32). TY medium results from the omission of glucose from the TGY formula. All cultures were grown under anaerobic conditions in anaerobic jars containing GasPak (BD) at 37°C.

TABLE 2. Primers used in this study

Primer	Primer sequence[a]	Positions[b]	Gene	Use[c]
CPP53	5′ GCGTCGACGAGATATGGTCTTTTAGATGG 3′	−333 to −312	*pilT* promoter	GUS
CPP55	5′ GCTGCAGCAGATGCTCCTTCTTTAACTG 3′	+28 to + 48	*pilT* promoter	GUS
CPP230	5′ GCGTCGACCTTGAAGATTTAGATAAGCCTC 3′	+19 to + 41	*pilD* promoter	GUS
CPP231	5′ GCTGCAGCCTTCCAATTATTAATCCAAATAA 3′	−361 to −341	*pilD* promoter	GUS
CCP-F	5′ AACTAGGATATAGACCTAAT 3′	+172 to +192	*ccpA*	MP
CCP-R	5′ TGATCCCATATCATACATTG 3′	+876 to +896	*ccpA*	MP
KO-F	5′ CTGGAGTGTCAATAGCAAC 3′	+34 to +53	*ccpA*	PROBE
KO-R	5′ TCTCCTAGTGATGAACTCAT 3′	+366 to +386	*ccpA*	PROBE
CPP265	5′ ATATCCATCAAGTTCATCTATAGAG 3′	−505 to −481	*ccpA*	COMP
CPP266	5′ TATGTTACCTAATGATTATGCATT 3′	+1012 to +1036	*ccpA*	COMP
P1	5′ ATGCTGATTACTCAGAAGCT 3′	−774 to −754	*ccpA* upstream	PCR
P2	5′ CTCATAAGCCCTTGATGAAC 3′	+1461 to +1484	*ccpA* downstream	PCR
M13-F	5′ GTA AAA CGA CGG CCA GT 3′		pUC18 vector	PCR
M13-R	5′ CAGGAAACAGCTATGAC 3′		pUC18 vector	PCR

[a] Restriction sites that have been added are underlined.
[b] The nucleotide position numbering begins from the first codon and refers to the relevant position within the respective gene sequence (36).
[c] GUS, construction of plasmid for β-glucuronidase assay; MP, construction of mutator plasmid; PROBE, construction of DNA probe for southern blot analysis; COMP, construction of complementing plasmid.

Motility assays. *C. perfringens* strains were grown overnight in FTG at 37°C, and 300 μl of this culture was inoculated and propagated in TGY for 5 h at the same temperature. Next, 1 ml of culture was centrifuged and concentrated twofold. Five microliters of the concentrated cell suspension was spotted onto a predried (1 h at 37°C) BHIA, TGY agar (TGYA), or TY agar (TYA) plate. All plates were supplemented with 0.7% agar. The inoculated plates were then incubated anaerobically for 48 to 96 h at 37°C. Photographs of the plates were taken with a Canon Power Shot SD550 digital camera.

Construction of *gusA* fusion plasmids and the β-glucuronidase assay. The PCR-amplified product carrying the upstream region of *pilD* or *pilT* was first cloned into the pCR-XL-TOPO vector by using a TOPO-XL cloning kit (Invitrogen). Briefly, the DNA fragment carrying the promoter region of *pilT* or *pilD* from SM101 or strain 13 was amplified by PCR using primers CPP53/CPP55 or CPP230/CPP231, respectively (Table 2). The SalI site was incorporated into the forward primer and the PstI site into the reverse primer of each primer pair. These PCR products were then cloned into the pCR-XL-TOPO vector. The recombinant clones carrying the expected DNA fragment were confirmed by restriction enzyme digestion, PCR analysis, and then DNA sequencing. The SalI-PstI fragments carrying the promoter region of *pilD* or *pilT* from pCR-XL-TOPO clones were then recloned into the SalI/PstI sites of pMRS127 to create *pilD-gusA* or *pilT-gusA* fusion constructs derived from either strain SM101 or strain 13. These reporter plasmids were then introduced by electroporation and Cm^r selection (8) into the corresponding wild-type *C. perfringens* strains 13 and SM101 and the isogenic derivates deficient in CcpA.

The strains carrying the *gusA* fusions were grown overnight in FTG at 37°C, and 150 μl of each culture was inoculated into TY and TGY. At various time points, 1 ml of each culture was centrifuged for 2 min at 9,000 rpm, and the pellet was stored frozen at −20°C until used. The cell pellets were resuspended with 1 ml of buffer Z (8.54 g of Na_2HPO_4, 5.5 g of $NaH_2PO_4 \cdot H_2O$, 0.75 g of KCl, 0.25 g of $MgSO_4$, and 1.4 ml of β-mercaptoethanol · $7H_2O$, pH 7, per liter) (13, 28). Adequate aliquots of the resuspended cells were brought to a final volume of 730 μl with buffer Z. Next, 10 μl of 10 mg/ml lysozyme was added and the mixture was incubated for 30 min at 37°C, followed by the addition of 10 μl 10% Triton X-100 (Sigma). The enzymatic reactions were initiated by adding 100 μl of 6 mM 4-nitrophenyl β-D-glucuronide (Sigma). After 15 min of incubation at 37°C, the reaction was stopped by adding 150 μl of 1 M Na_2CO_3. The absorbance was measured at 405 nm, and the β-glucuronidase activity was calculated using the following equation: (A_{405} × 1,000)/(optical density at 600 nm [OD_{600}]pls cross chk inf or sup, edi file not provided × culture volume [in milliliters] × time [in minutes]) (19).

Insertional inactivation of *ccpA* gene in strain 13. To disrupt *ccpA* in strain 13, an internal 760-bp fragment of the *ccpA* gene was amplified by PCR using primers CCP-F and CCP-R (Table 2) and cloned into the SmaI site of pUC18 to create pKO1. For selection, an erythromycin resistance cassette (*ermBP*) was ligated into the HincII site of pKO1, creating pKO2. The plasmid pKO2 (which has no origin of replication for *C. perfringens*) was transformed into strain 13 by electroporation and Em^r selection. One Em^r clone (KO13) was analyzed (see Fig. S1 in the supplemental material) for correct integration by a single crossover event involving homologous recombination of the suicidal mutator plasmid (pKO2) on *ccpA* and utilized in the present study.

The insertional disruption of wild-type *ccpA* in KO13 was first demonstrated by PCR analysis of DNA isolated from the mutant (see Fig. S1 in the supplemental material). As expected, a 1.6-kb product was amplified from KO13 DNA by using primers P1 and M13F and a 2.5-kb product by using primers P2 and M13R. However, no PCR product was obtained with either P1 and M13R or P2 and M13F. These PCR results are consistent with the suicidal mutator plasmid pKO2 having been inserted into the wild-type *ccpA* gene in KO13. Southern blot analyses showed that a 2.4-kb HindIII DNA fragment from wild-type strain 13 hybridized with our *ccpA*-specific probe. However, two hybridizing bands, of 2.9 and 4.3 kb, were observed with DNA from mutant strain MO13. This profile is consistent with the expected result since the inserted pKO2 plasmid has a HindIII site.

Southern blot analysis. A 350-bp internal *ccpA* DNA fragment was amplified from strain 13 by PCR using primers KO-F and KO-R (Table 2) and labeled with alkaline phosphatase using the Gene Images AlkPhos direct labeling and detection system (Amarsham Bioscience) (28, 44). Isolated *C. perfringens* DNA samples, prepared as described previously (8, 38), were digested with HindIII, separated by electrophoresis on 1% agarose gels, and transferred by Southern blotting. The blot was hybridized with the AlkPhos-labeled *ccpA* probe, and the hybridized probe was then detected by CDPstar chemiluminescence (Amersham Bioscience).

Construction of the CcpA-complementing plasmid pIH100. A 1,539-bp fragment containing the *ccpA* open reading frame and its 450-bp upstream region was amplified by PCR using primers CPP265 and CPP266 (Table 2) and then cloned into pCR-TOPO-XL (Invitrogen) to generate pCcpA-comp-XL. Next, the ~1.5-kb KpnI/XbaII fragment was cloned into the KpnI/XbaI sites of shuttle vector pJIR750 to generate the *ccpA*-complementing plasmid pIH100.

RESULTS

Glucose represses the gliding motilities of wild *C. perfringens* strains isolated from human and animal infections. A recent study demonstrated TFP-dependent gliding motility in three human-derived *C. perfringens* strains for which genome sequences have been previously determined (41). TFP-dependent gliding motility constitutes an important bacterial behavior also known as twitching (14, 15, 24). Taking into account that the referred study (41) was limited to the analysis of only three strains, all of human origin, when there exists a great diversity of *C. perfringens* isolates causing diverse infections (i.e., gas gangrene, food poisoning, antibiotic-associated diarrhea, etc.) in human beings and animals, we considered it of

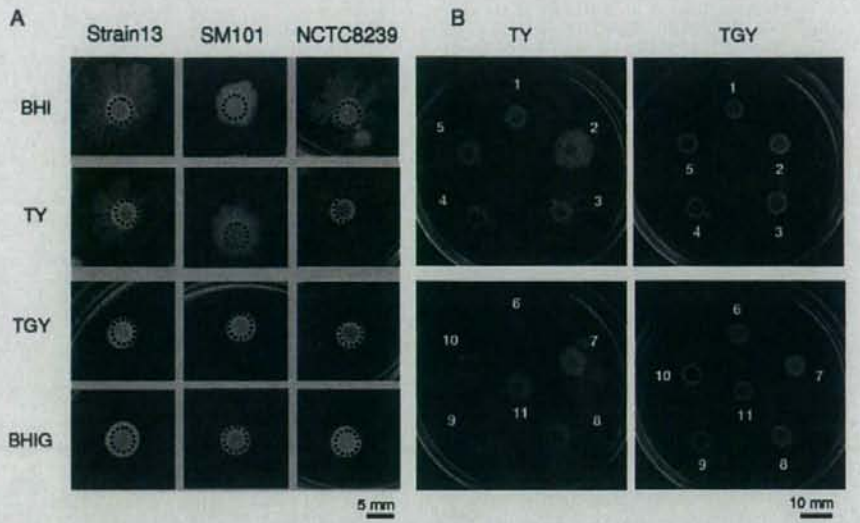

FIG. 1. Glucose represses the gliding motilities of *C. perfringens* strains isolated from different mammalian hosts. (A) Gliding phenotypes of the three genome-sequenced human pathogen *C. perfringens* strains 13, SM101, and NCTC8239. Gliding was developed after inoculation of a 5-μl drop of a concentrated middle-log-phase culture of the corresponding strain on BHIA or TYA medium with or without 2% glucose supplementation. Top-bottom photographs were taken after 72 h of anaerobic incubation at 37°C. BHIA, TYA medium without glucose; BHIG and TGY, media supplemented with 2% glucose. Black dotted circles show the diameters of the initial inoculation spots (see Materials and Methods for details). (B) Gliding phenotypes of a collection of human and animal pathogenic *C. perfringens* strains: 1, NB16; 2, JGS1818; 3, 294442; 4, NCTC 10239; 5, 317206; 6, AHT327; 7, B11; 8, B41; 9, F5603; 10, F4969; and 11, AHT2911 (see Table 1 for the origin and type of infection produced for each pathogenic strain).

interest to evaluate whether gliding motility was an intrinsic and general property of wild and undomesticated *C. perfringens* isolates. To this end, we performed a gliding motility analysis on a collection of 17 different pathogenic human- and animal-derived *C. perfringens* strains (including those strains whose gliding behavior was previously reported) (Table 1). In our study, motility is defined as the ability of cells to spread away from the edge of inoculation point by at least 0.4 cm in a curved flare pattern after 72 h at 37°C. When culture aliquots (see Materials and Methods for details) of strains 13, SM101, and NCTC8239 were spotted onto BHIA or TYA plates, the pattern of colony translocation was similar to that of the gliding motility previously observed (41), showing a distinctive curved flare pattern (Fig. 1A). Interestingly, both on TGYA and on BHIGA plates (which contained 2% glucose), the spotted cultures of strains 13, SM101, and NCTC8239 remained in the inoculation point, indicating that gliding motility was inhibited. In addition, we noted that the degree of motility was more evident on TYA than on the BHIA that was used in the previous study (41) (Fig. 1A and data not shown). Therefore, all subsequent motility experiments were conducted using TYA plates.

When the gliding motility assay was performed on the entire collection of *C. perfringens* isolates (Table 1), all the strains exhibited full proficiency in social gliding motility on TYA plates. Gliding motility was, in contrast, completely blocked in the presence of glucose (Fig. 1B and data not shown). Therefore, taking into consideration that glucose is a known inhibitor of other bacterial social behaviors, such as sporulation (28, 30) and biofilm formation (39), we concluded that the glucose added to the BHIA and TYA plates, yielding BHIG and TGYA, respectively, was responsible for the repressive effect on the gliding motilities of all the surveyed *C. perfringens* isolates.

To determine how gliding motility was affected by different glucose levels, a glucose gradient was generated on a TYA plate (see Materials and Methods). Five microliters of a concentrated middle-log phase culture of the food poisoning strain SM101 was inoculated at various positions distributed along the TYA glucose concentration testing plate (see Materials and Methods). As observed in Fig. 2A, the extent of gliding motility exhibited by the pathogenic food poisoning SM101 strain was inversely proportional to the glucose concentration; as the concentration of glucose decreases, the extent of gliding motility increases.

To determine the minimum concentration of glucose required to inhibit gliding motility, five different concentrations of the sugar were independently assayed: 0.1%, 0.25%, 0.5%, 1%, and 2%. As shown in Fig. 2B, at a glucose concentration of 1%, no gliding motility was observed in the gas gangrene producer strain 13 or in the food poisoning isolate NCTC8239. In contrast, these two strains were able to glide slightly on TYA plates supplemented with 0.5% glucose. No inhibition of gliding motility was observed when these strains were spotted on TYA plates supplemented with 0.25% and 0.1% glucose (Fig. 2B and data not shown). Therefore, glucose repression of social gliding motility in *C. perfringens* was concentration dependent and apparently triggered at a glucose concentration of 0.5%.

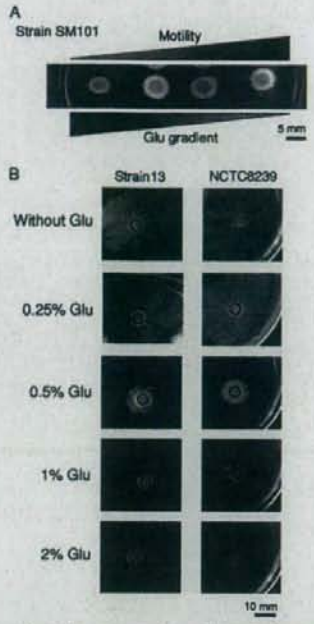

FIG. 2. Dose-dependent repressive effect of glucose (Glu) on *C. perfringens* gliding proficiency. (A) Glucose gradient effect on the gliding motility of the enterotoxigenic *cpe*$^+$ food poisoning *C. perfringens* strain SM101. One-third of a TYA plate was cut out and replaced with 7 ml of melted TGYA medium, which contained 2% glucose (see Materials and Methods and elsewhere in text for details). After solidification of the added TGYA, a natural glucose gradient was generated (shown from left to right) due to the diffusion of glucose molecules from the TGYA section (which contained 2% added glucose) to the TYA portion (which contained 0% added glucose) of the plate. (B) Evaluation of the minimum glucose concentration required to inhibit gliding proficiency of the food poisoning and gas gangrene producer strains NCTC8239 and 13. For panels A and B, strains were grown on TYA plates as indicated in Fig. 1 and supplemented with glucose as shown in the figure. Top-bottom photographs were taken after 72 h of anaerobic incubation at 37°C.

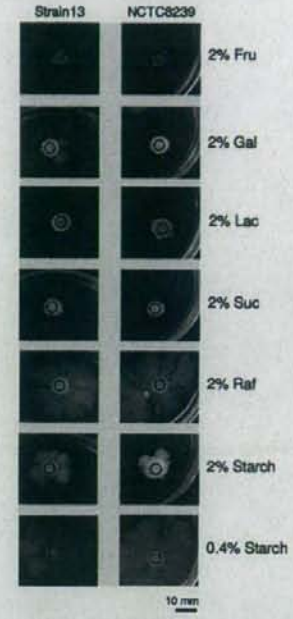

FIG. 3. Effects of simple and complex carbohydrates on *C. perfringens* gliding motility. Rapidly metabolized carbohydrates (Fru, fructose; Gal, galactose; Lac, lactose; Suc, sucrose) and complex carbohydrates (Raf, raffinose) commonly used to enhance sporulation and CPE production in Spo0A-proficient *C. perfringens* strains were assayed for their abilities to affect gliding motility. The gliding phenotypes of the gas gangrene producer and Spo0A-deficient strain 13 and the Spo0A-proficient and food poisoning strain NCTC8239 are shown. Top-bottom photographs were taken after 96 h of anaerobic incubation at 37°C on TYA plates supplemented with the corresponding concentrations of sugar as indicated.

Carbon catabolite repression of *C. perfringens* gliding motility. In order to determine if the observed inhibitory effect of glucose on gliding motility was a general phenomenon of carbon catabolite regulation (repression), other readily metabolized carbohydrates, such as galactose, fructose, lactose, and sucrose, were tested. The motilities of strains NCTC8239 (food poisoning) and 13 (gas gangrene) were inhibited when these strains were grown on plates containing 2% of either fructose, galactose, lactose, or sucrose (Fig. 3). Next, we analyzed the effects on gliding of complex carbohydrates (e.g., raffinose and starch), which are slowly metabolized but are required for efficient sporulation of *C. perfringens* and for *C. perfringens* enterotoxin (CPE) production (17, 18). When 2% raffinose was added to TYA plates, no inhibition of gliding motility was observed (Fig. 3). With 2% starch, the extents of motility in both strains (13 and NCTC8239) were suppressed to a minor degree, although gliding was not affected in the presence of 0.4% starch (Fig. 3). When similar experiments were performed on the rest of the *C. perfringens* isolates listed in this work (Table 1), no gliding motility was observed for all tested strains grown on TYA plates supplemented with 2% fructose, galactose, lactose, or sucrose, while gliding motility was observed with 2% raffinose supplementation. However, on TYA plates supplemented with 2% starch, all tested strains were nonmotile on the agar surface, with the exception of the strains NCTC10239 (food poisoning), which exhibited partial gliding motility, and JGS1807 (diarrheic pig), which was highly motile even in the presence of 2% starch (data not shown). The overall results indicated that the complex carbohydrates raffinose and starch did not affect gliding motility at the concentrations routinely used (2% and 0.4%, respectively) for *C. perfringens* spore formation and CPE production (17, 18, 28). More importantly, we demonstrate for the first time that *C. perfringens* gliding motility is subject to carbon catabolite repression.

Kinetics of TFP-dependent gliding motility in *C. perfringens*. Proficiency in surface-associated motility is an important feature of many human and animal pathogens (2, 10, 14, 21, 24). In the cases of virulent and invasive *C. perfringens* isolates, an efficient mechanism of translocation on solid or semisolid surfaces could be favorable for escape from host defenses and for rapid dissemination of the infection (i.e., an aggressive gan-

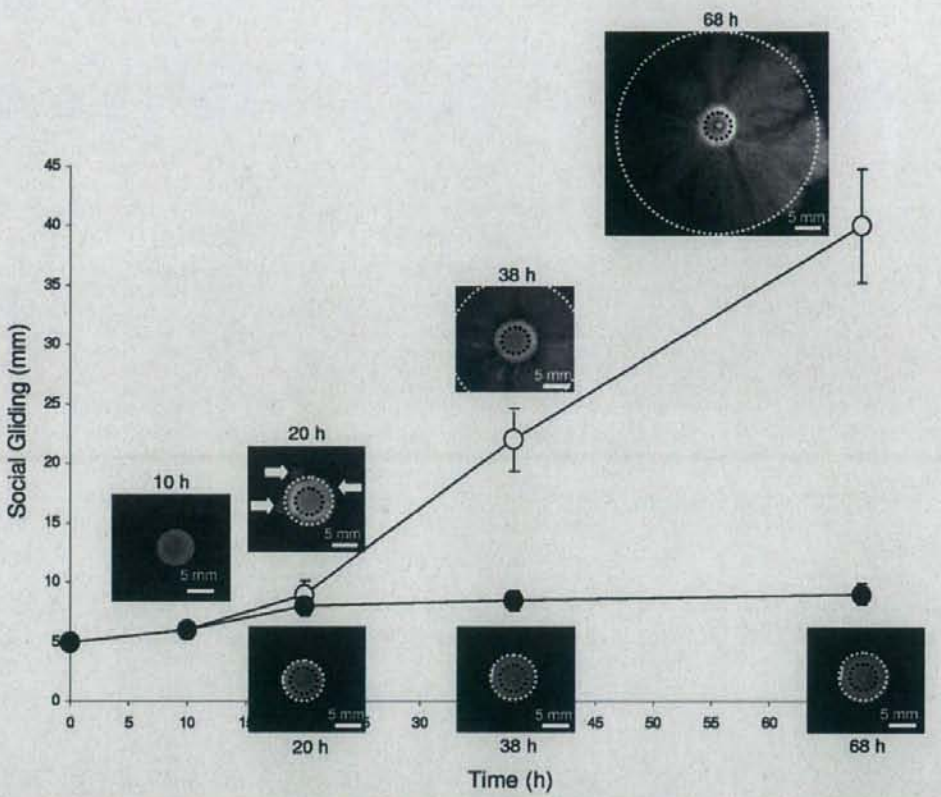

FIG. 4. Kinetics of gliding development of the gas gangrene producer *C. perfringens* strain 13 in the absence and presence of added glucose. Five microliters of a concentrated middle-log-phase culture of strain 13 grown in TY broth was inoculated in the center of each 100-mm petri dish, containing TYA medium with or without supplementation with 2% glucose. Inoculated petri dishes were anaerobically incubated at 37°C, and gliding proficiency was recorded at different times, measuring the distance traveled (in mm) from the initial inoculation point (black dotted circles) to the edge of the expanding colony (white dotted circles). Open and closed symbols represent the experiments performed in the absence and the presence of 2% added glucose, respectively. White arrows indicate the onset (under the influx of unknown signals; see text for details) of gliding development. The onset of gliding was observed only in TYA plates without glucose supplementation, while in the presence of glucose, gliding was never initiated. Photographs are representative of six independent experiments, and plotted values are the averages for those repetitions.

grene can progress at a rate of 1 cm h^{-1}). Therefore, we consider it of interest to characterize the kinetics and efficiency of the gliding motility of strain 13 (gas gangrene producer) on semisolid TYA plates in the absence and presence of added glucose. As observed in Fig. 4, it is possible to visualize two clear phases of colony growth and expansion. Initially, the growing colony expanded on the TYA surface from the inoculation point at a rate comparable to the speed of colony expansion expected from nonswimming bacteria. During the first 20 h of incubation, the size of the growing colony was evenly increased by a factor of 1.75 as a consequence of cell division, reaching a speed of colony spreading of approximately 125 $\mu m\ h^{-1}$ (Fig. 4 and data not shown). After this initial phase of even colony spreading, a striking change occurred: social gliding was initiated by groups of cells located at the edge of the colony (see marked burgeoning cells in Fig. 4 at a developmental time of 20 h). After the appearance of these first signs of active surface gliding motility (the emergence of up-and-coming cells from the budding sites), a robust and uniform gliding was strongly induced, reaching a maximal speed of 600 to 700 $\mu m\ h^{-1}$ (Fig. 4), a value for gliding speed comparable to the average values (200 $\mu m\ h^{-1}$ to 1,000 $\mu m\ h^{-1}$) for social gliding and twitching speed previously reported for other microorganisms (10, 14, 24).

Interestingly, in the presence of 2% glucose, gliding motility was not generated even after long incubation times (Fig. 4 and data not shown). The morphology of the *C. perfringens* colony developed on TYA plates supplemented with glucose (gliding-deficient phenotype) was quite similar to the morphology of the colony developed on TYA plates without glucose supplementation just before the onset of active gliding; it was also very similar to that of the central part of a mature colony that has glided for more than 40 h on TYA plates (Fig. 4 and data not shown). These observations indicate that glucose and other sugars (data not shown) did not affect the initial phase of vegetative colony spreading. However, they do show that the sugar completely blocked (with carbon catabolite repression) the onset of the

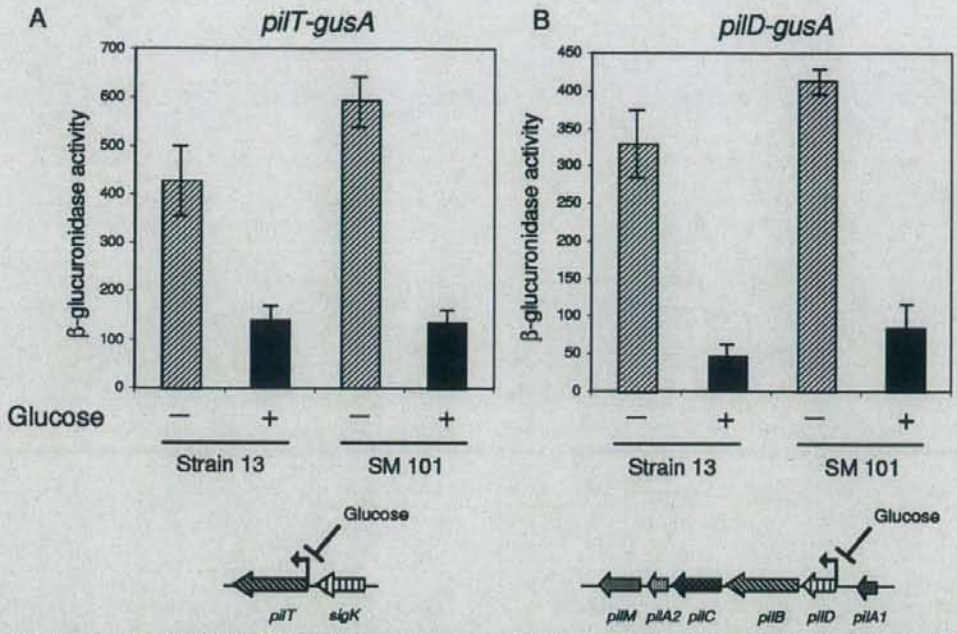

FIG. 5. Glucose represses *pilT* and *pilD* transcription in gas gangrene and food poisoning *C. perfringens* strains. Transcription of *pilT* (A) and *pilD* (B) promoters measured by a β-glucuronidase assay of *C. perfringens* strains 13 and SM101, harboring reporter *pilT-gusA* (A) and *pilD-gusA* (B) transcriptional fusions. Strains were grown on TY broth with or without the addition of 1% glucose as indicated in the figure (+ or −, respectively). Accumulated β-glucuronidase activity was measured after 30 h of growth. A representative result from three independent assays is shown. Gene arrangements of *pilT* (A) and *pilD* (B) chromosomal regions in *C. perfringens* strains 13 and SM101 are shown at the bottom of the figure, with the repressive effects of glucose on gene transcription indicated (see text for details).

second phase of surface translocation, which relied on the development of active gliding.

Effects of glucose on *pilT* and *pilD* expression of gas gangrene and food poisoning-producing *C. perfringens* strains. The recent study of Varga et al. demonstrated that the gliding of *C. perfringens* strain 13 depended on the products of *pilT* and *pilC*, which are required for TFP assembly (41). The *pilT* mutant of strain 13 does not spread out from the inoculation spot as the wild type does, and no pili were detected using field emission-scanning electron microscopy (41). Since glucose and other readily metabolized carbohydrates completely suppressed gliding motility in all the surveyed *C. perfringens* strains (Table 1) that we analyzed (Fig. 1 to 4 and data not shown), we considered the scenario where the transcription of *pil* genes might be affected by carbon catabolite repression. Therefore, to test this hypothesis, we measured the expression levels of two other genes required for TFP-dependent motility, *pilD* and *pilT*, in TY medium with and without glucose supplementation (Fig. 5). The β-glucuronidase *pilD-gusA* and *pilT-gusA* reporter fusions were introduced separately into strains 13 and SM101 by DNA electroporation, and *pil*-driven β-glucuronidase activity was assayed (see Materials and Methods for details). There were no significant differences in the growth of strains carrying the *pil-gusA* fusions in medium with or without added glucose (data not shown), although the final cellular yield was slightly higher in TY medium supplemented with glucose than in nonsupplemented TY medium (data not shown). Interestingly, in the presence of 1% glucose, there were dramatic down-regulations of *pilD* and *pilT* promoter activities in both *C. perfringens* strains (Fig. 5). The expression levels of *pilT* were reduced by 60% in the gas gangrene producer strain 13 and by 75% in the food poisoning isolate SM101 when these strains were grown in the presence of 1% glucose (Fig. 5A). Similarly, significant reductions in *pilD-gusA* expression were observed in cultures of strains 13 (~80% reduction) and SM101 (~75% reduction) when these strains were grown in the presence of 1% glucose in comparison with their expression levels in the absence of glucose (Fig. 5B). These results demonstrated that glucose strongly down-regulates the expression levels of the *pilT* and *pilD* genes. They also suggest that the inhibitory effect of carbon catabolite regulation on gliding motility took place, at least partially, at the level of TFP expression.

Dual role of the carbon catabolite protein CcpA in *C. perfringens* gliding motility. It is known that catabolite control protein A (CcpA) plays a key role in low-G+C-content, gram-positive bacteria, interconnecting carbon metabolism with several cellular responses, such as virulence, spore formation, and biofilm development (39, 43). In *C. perfringens*, CcpA is required for efficient sporulation and expression of the enterotoxin (CPE) that is responsible for the symptoms of food poisoning and diarrhea in humans and animals (42). Due to the observed repressive effect of glucose on the expression levels of *pil* genes (Fig. 5) that are essential for the ability of *C. perfringens* to glide on a solid substrate (41), we were tempted to

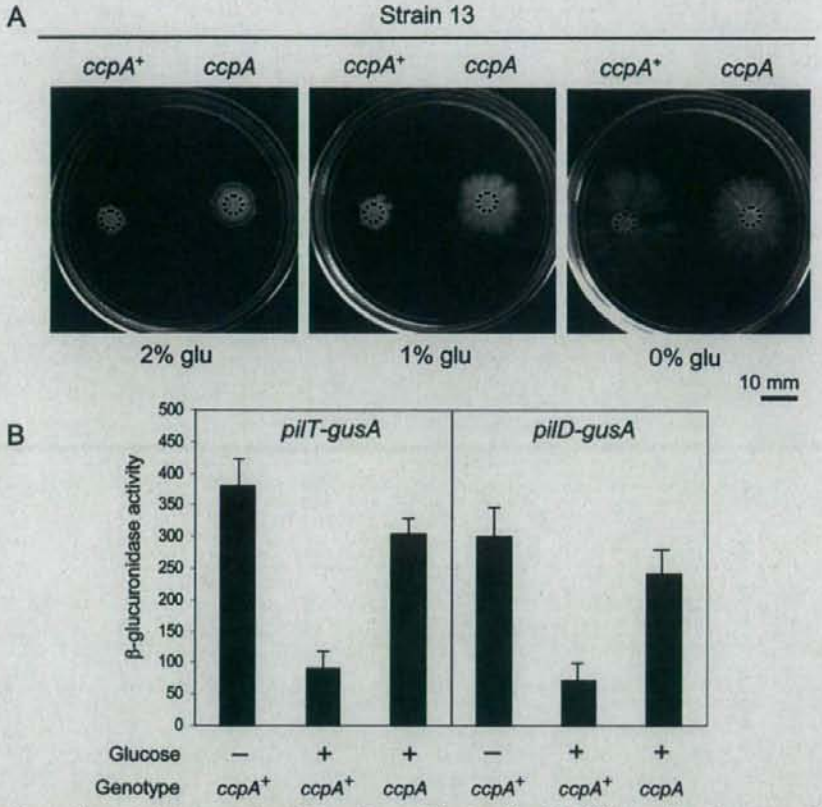

FIG. 6. CcpA mediates carbon catabolite repression of *C. perfringens* gliding motility. (A) Gliding motility phenotypes of the CcpA-proficient (*ccpA*$^+$) *C. perfringens* strain 13 and its isogenic CcpA-deficient derivate KO13 (see Materials and Methods for details). A motility assay was performed according to the protocol described in the above figure legends. Top-bottom photographs were taken after 40 h of anaerobic incubation on TYA plates supplemented or not supplemented with glucose (glu) as indicated in the figure. Black dotted circles indicate the initial sizes of the colonies immediately after drop inoculation. (B) Expression of *pilT-gusA* and *pilD-gusA* reporter fusions in *ccpA*$^+$ and *ccpA* cultures of isogenic *C. perfringens* strains 13 and KO13 grown for 30 h on TY broth in the absence (−) or presence (+) of 1% glucose. β-Glucuronidase activity was calculated as indicated in Fig. 5. For panels A and B, a representative set of results obtained from five independent experiments is shown.

analyze whether CcpA has a role in the carbon catabolite repression of *C. perfringens* gliding motility. To explore this possibility, we constructed a *C. perfringens ccpA* mutant strain (see Materials and Methods and Fig. S1 in the supplemental material) to assay the gliding phenotypes and the activities of TFP genes (*pilT* and *pilD*) of isogenic *ccpA*$^+$ and *ccpA C. perfringens* strains grown in the presence or absence of added glucose. When gliding proficiency was evaluated in the presence of 1% and 2% glucose, the CcpA-proficient strain 13 was, as expected, unable to move at both sugar concentrations, remaining situated at the point of inoculation (round and smooth colony morphology). In contrast, the isogenic *ccpA* mutant derivate KO13, deficient in CcpA production and inoculated on the same plates, was able to retain more than 50% of its gliding ability in the presence of 1% glucose and also showed a low but perceptible and reproducible level of gliding proficiency on TYA plates supplemented with 2% glucose (Fig. 6A). Under similar conditions, no gliding motility was observed in the presence of 1% glucose with the *ccpA* mutant strain harboring the CcpA-complementing plasmid pIH100 (Table 1 and data not shown), suggesting that functional CcpA was required for carbon catabolite repression of *C. perfringens* social gliding motility.

In order to further confirm the role of CcpA in carbon catabolite repression of *C. perfringens* gliding motility, we compared the expression levels of *pilT* and *pilD* in isogenic CcpA-proficient and CcpA-deficient *C. perfringens* cultures grown in TY broth plus/minus 1% glucose. As shown in Fig. 6B, the CcpA-deficient cultures, but not the cultures that express CcpA, showed active expression of *pilT* and *pilD* in the presence of glucose at almost the same level observed for wild-type cultures grown in the absence of glucose. Collectively, these results demonstrate that CcpA was actively involved in the carbon catabolite repression of *C. perfringens* gliding motility and the glucose-induced down-regulation of TFP biosynthetic genes.

An intriguing observation was that the gliding ability of the CcpA-deficient *C. perfringens* strain KO13 grown in the ab-

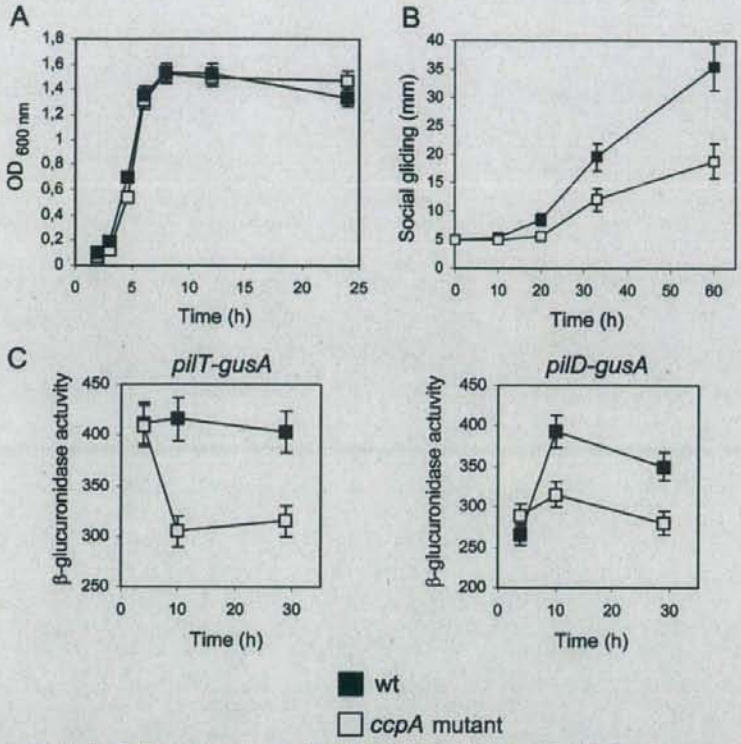

FIG. 7. CcpA has a novel catabolite-independent positive role in *C. perfringens* gliding motility. (A) Growth curves of the *ccpA*$^+$ *C. perfringens* strain 13 and its isogenic *ccpA* derivate KO13. Growth was monitored over time, measuring the OD_{600}s of both cultures developed on TY broth at 37°C. A representative set of results obtained from five independent experiments is shown. Closed symbols, wild type (wt); open symbols, *ccpA* mutant. (B) Kinetics of gliding motility of strain 13 (wt) and its isogenic CcpA-deficient derivate KO13 (*ccpA* mutant) developed on TYA plates without sugar supplementation. Gliding was recorded as indicated in Fig. 4. Average values of gliding obtained from five independent experiments are plotted. (C) Requirement of CcpA activity for full expression of *pilT* and *pilD* genes of *C. perfringens* strain 13 grown on TY broth without glucose supplementation. β-Glucuronidase activities driven from CcpA-proficient and CcpA-deficient *C. perfringens* cultures (strains 13 and KO13, respectively) harboring reporter *pilT-gusA* (left) and *pilD-gusA* (right) transcriptional fusions are shown. The four cultures were grown on TY broth without addition of glucose; accumulated β-glucuronidase activity was measured at the times indicated in the figure. Closed and open symbols represent CcpA-proficient and CcpA-deficient isogenic cultures, respectively. A representative set of results obtained from five independent experiments is shown.

sence of sugar supplementation was delayed in comparison with the gliding proficiency of the wild-type (*ccpA*$^+$) strain 13 (see right panel, no added glucose, in Fig. 6A). This observation could uncover an additional, and unexpected, carbon-independent positive requirement of CcpA for full proficiency of *C. perfringens* in gliding motility. It is worth indicating that the slight but reproducible catabolite-independent positive effect of CcpA on social behaviors has been previously documented during biofilm formation in *Bacillus subtilis* (39) and spore development in *C. perfringens* (42). In these bacteria, the absence of CcpA activity was reflected in a low level of proficiency in biofilm development and spore formation in comparison with the abilities of the wild-type (CcpA-proficient) strains (39, 42).

We confirmed our hypothesis by quantifying the gliding developed by the *ccpA*$^+$ (strain 13) and its isogenic *ccpA* mutant derivate on TYA plates in the absence of glucose supplementation. Previously, we determined that introduction of the *ccpA* mutation in strain 13 did not affect its growing ability and the final cellular yield after growth in liquid TY medium (Fig. 7A). In contrast to what occurred in broth, where the growth phenotypes of the CcpA-proficient and CcpA-deficient cultures were the same, we observed clear differences in the speed and kinetics of gliding between the *ccpA*$^+$ and *ccpA* strains. The gliding proficiency of the *ccpA* mutant strain showed a reduced speed compared with the velocity of gliding of the wild-type strain: 250 $\mu m\ h^{-1}$ and 670 $\mu m\ h^{-1}$ for the CcpA-deficient and CcpA-proficient strains, respectively (Fig. 7B). Also, the gliding of the *ccpA* mutant strain stopped before the gliding of the wild-type strain did (Fig. 6A, right, and 7B). These observations strongly suggest a novel and overlooked positive role for CcpA in the proficiency of gliding motility of *C. perfringens* in the absence of sugar supplementation. To confirm this conclusion, we measured the expression levels of *pilD* and *pilT* (whose products are essential for TFP-dependent gliding motility) in wild-type and CcpA-deficient *C. perfringens* cultures